THE JOURNAL OF BIOLOGICAL CHEMISTRY VOL. 289, NO. 37, pp. 25907–25924, September 12, 2014
© 2014 by The American Society for Biochemistry and Molecular Biology, Inc. Published in the U.S.A.

Multifunctional Roles for the Protein Translocation Machinery in RNA Anchoring to the Endoplasmic Reticulum*[S]

Received for publication, May 13, 2014, and in revised form, July 21, 2014 Published, JBC Papers in Press, July 25, 2014, DOI 10.1074/jbc.M114.580688

Sujatha Jagannathan[‡1], Jack C.-C. Hsu[§1], David W. Reid[§], Qiang Chen[‡], Will J. Thompson[¶], Arthur M. Moseley[¶], and Christopher V. Nicchitta[‡§2]

From the Departments of [‡]Cell Biology and [§]Biochemistry and the [¶]Duke Proteomics Core Facility, Duke University Medical Center, Durham, North Carolina 27710

Background: ER-localized mRNAs are anchored to the ER via their functional engagement with translocon-bound ribosomes.
Results: Ribosome-engaged mRNAs are ER-bound through distinct and mRNA-selective mechanisms.
Conclusion: Multiple ER membrane proteins, including the Sec61 complex, display RNA binding activity and anchor select mRNAs to the ER.
Significance: These data reveal new functions for the translocation machinery and advance understanding of RNA localization to the ER.

Signal sequence-encoding mRNAs undergo translation-dependent localization to the endoplasmic reticulum (ER) and at the ER are anchored via translation on Sec61-bound ribosomes. Recent investigations into the composition and membrane association characteristics of ER-associated mRNAs have, however, revealed both ribosome-dependent (indirect) and ribosome-independent (direct) modes of mRNA association with the ER. These findings raise important questions regarding our understanding of how mRNAs are selected, localized, and anchored to the ER. Using semi-intact tissue culture cells, we performed a polysome solubilization screen and identified conditions that distinguish polysomes engaged in the translation of distinct cohorts of mRNAs. To gain insight into the molecular basis of direct mRNA anchoring to the ER, we performed RNA-protein UV photocross-linking studies in rough microsomes and demonstrate that numerous ER integral membrane proteins display RNA binding activity. Quantitative proteomic analyses of HeLa cytosolic and ER-bound polysome fractions identified translocon components as selective polysome-interacting proteins. Notably, the Sec61 complex was highly enriched in polysomes engaged in the translation of endomembrane organelle proteins, whereas translocon accessory proteins, such as ribophorin I, were present in all subpopulations of ER-associated polysomes. Analyses of the protein composition of oligo(dT)-selected UV photocross-linked ER protein-RNA adducts identified Sec61α,β and ribophorin I as ER-poly(A) mRNA-binding proteins, suggesting unexpected roles for the protein translocation and modification machinery in mRNA anchoring to the ER. In summary, we propose that multiple mechanisms of mRNA and ribosome association with ER operate to enable an mRNA transcriptome-wide function for the ER in protein synthesis.

All eukaryotic cells localize secretory and membrane protein-encoding mRNAs to the endoplasmic reticulum (ER),[3] the entry portal to the secretory pathway (1–3). ER-directed RNA localization operates on a remarkably large scale, where up to 50% of the genome can encode topogenic signal-bearing proteins (4), and by a mechanism quite distinct from that established for more prominent examples of RNA localization (5, 6). In the majority of these latter cases, RNA localization occurs via motor protein-based transport of translationally repressed, "zip code" element-encoding mRNAs to the cell periphery (5, 6). RNA localization to the ER, in contrast, utilizes a co-translational mechanism, the signal recognition particle (SRP) pathway, which does not require motor protein-based transport and uses localization information encoded in the nascent protein rather than the mRNA (3, 7, 8).

Although SRP pathway function in RNA localization to the ER is well established, recent investigations into the subcellular partitioning of mRNAs and their translation, as well as the biochemical basis of their ER association, have revealed an unexpected complexity in the ER-associated mRNA transcriptome (9–12). Notably, the near entirety of the mRNA transcriptome undergoes translation on ER-bound ribosomes, and ER-associated mRNAs differ in their requirement for ribosome engagement as the primary mechanism of their ER association (12–15). By the latter criterion, one class of mRNAs has distinguished itself: the mRNAs encoding resident proteins of the endomembrane organelles. This mRNA cohort shares a number of molecular characteristics, including translation- and sig-

* This work was supported, in whole or in part, by National Institutes of Health Grant GM101533 (to C. V. N.). This work was also supported by a bridge-funding award from the Duke University School of Medicine (to C. V. N.). The DeltaVision system was purchased with funding from National Institutes of Health, NCRR, Shared Instrumentation Grant 1S10RR027528-0.
[S] This article contains supplemental Tables S1–S3.
[1] Both authors contributed equally to this work.
[2] To whom correspondence should be addressed: Dept. of Cell Biology, Box 3709, Duke University Medical Center, Durham, NC 27710. Tel.: 919-684-8948; Fax: 919-684-5481; E-mail: christopher.nicchitta@duke.edu.

[3] The abbreviations used are: ER, endoplasmic reticulum; SRP, signal recognition particle; RBP, RNA-binding protein; RM, rough microsome(s); B2M, β_2-microglobulin; HLB, hydrophile-lipophile balance; CHAPSO, 3-[(3-cholamidopropyl)dimethylammonio]-2-hydroxy-1-propanesulfonic acid; BrS, Tris/Brij-sensitive; BrR, Tris/Brij-resistant; qRT-PCR, quantitative RT-PCR; EJC, exon-junction complex; mRNP, messenger ribonucleoprotein.

nal peptide-independent ER localization, ribosome-independent anchoring to the ER, and a uniquely high ER enrichment (12, 13, 15). Importantly, these findings are not unique to mammalian cells; translation-independent localization of mRNAs to the yeast ER as well as the *Escherichia coli* inner membrane has also been reported (16–18).

At present, little is known regarding the *in vivo* mechanisms of mRNA localization and anchoring to the ER (11, 19). Presumably, direct mRNA anchoring to the ER membrane would require RNA-binding proteins (RBPs), which are known to serve diverse functions in RNA localization, translational regulation, and stability (20, 21). Indeed, recent studies have identified ribosome receptor RRBP1 (p180), a coiled-coil multidomain ER-resident membrane protein, as a general ER-poly(A) mRNA-anchoring protein (14, 22). p180 is multifunctional; as a microtubule-binding protein, it participates in the dynamic regulation of ER distribution in the cell, and it has been shown to enhance ribosome loading onto selected mRNAs and to regulate the stability of ER-associated mRNAs (23–27). p180 is reported to bind mRNAs nonspecifically, however, and so the question of how mRNAs undergo selective association with the ER membrane remains largely unanswered.

Here we used biochemical, genomic, optical imaging, and proteomic approaches to investigate mechanisms of mRNA-ER interaction in mammalian cells. These studies reveal a diversity of RNA anchoring processes, where cytosolic and secretory protein-encoding mRNAs display similar anchoring mechanisms and RNA-binding protein compositions, which are distinct from those utilized by endomembrane protein-encoding mRNAs. Intriguingly, proteomic analysis of native and photocross-linked ER-bound mRNAs identified components of the protein translocation machinery as ER-mRNA-anchoring proteins and suggests multifunctional roles for these proteins in the selective localization and anchoring of mRNAs to the ER.

EXPERIMENTAL PROCEDURES

Cell Culture and Sequential Detergent Fractionation—HeLa cells were maintained at 37 °C, 5% CO_2 in Dulbecco's modified Eagle's medium (DMEM; Mediatech) supplemented with 10% fetal bovine serum (FBS; Invitrogen). For detergent fractionations, cell cultures (75–90% confluence) were incubated on ice for 20 min in PBS/$MgCl_2$, 50 μg/ml cycloheximide (Sigma), to depolymerize the microtubule network (4 °C) and stabilize polyribosomes (cycloheximide). Cytosol fractions were obtained by treating cell monolayers with a plasma membrane permeabilization buffer (110 mM KCl, 25 mM K-HEPES, pH 7.4, 1 mM $MgCl_2$, 0.015% digitonin (Calbiochem), 0.1 mM EGTA, 40 units/ml RNAseOUT (Invitrogen), 1 mM DTT). The cytosol fraction was recovered, the cells were rinsed in a buffer of identical composition containing 0.004% digitonin, and the two fractions were combined. Subfractionation of the endoplasmic reticulum was performed by first treating the digitonin-extracted cell cultures with the indicated detergents at 10-fold critical micelle concentration, in a buffer consisting of 500 mM Tris-HCl, pH 7.0, 1 mM $MgCl_2$, 40 units/ml RNAseOUT, and 2 mM DTT, and subsequently extracting the cells in 2% dodecylmaltoside, 200 mM KCl, 25 mM K-HEPES, pH 7.4, 10 mM $MgCl_2$, 40 units/ml RNAseOUT, and 2 mM DTT (28–30).

Polyribosome Profiling and Negative Staining Electron Microscopy—Polyribosomes from the different subcellular fractions, prepared as described above, were resolved on 15–50% sucrose gradients and fractioned using a Teledyne/Isco gradient fractionator, as described previously (29, 30). To assess polysome translation status, cell cultures were supplemented with 150 μCi/ml [^{35}S]Met/Cys for 10 min in the presence or absence of cycloheximide and fractionated as above, and fractions were resolved by sucrose gradient centrifugation. Radiolabeled proteins were recovered by trichloroacetic acid (TCA) (10%, v/v) precipitation onto filter paper squares, boiled in 10% TCA, rinsed in cold 10% TCA, acetone-extracted, and dried, and radioactivity was measured by scintillation counting. Negative staining electron microscopy of the various polysome fractions was performed as described (31).

RNA Extraction and Quantitative RT-PCR—Total Samples were supplemented with Alien RNA (Life Technologies), and total RNA was extracted by acid guanidinium thiocyanate-phenol-chloroform extraction (32). Cell-equivalent quantities of total RNA were used to prepare cDNA using Moloney murine leukemia virus reverse transcriptase (Promega) and random hexamer primers (Roche Applied Science). Quantitative RT-PCR was performed on a 7900HT Sequence Detection System (Applied Biosystems) using Power SYBR® Green PCR mastermix (Applied Biosystems) and the following primers: GRP94, CTGGAAATGAGGAACTAACAGTCA (forward) and TCTTCTCTGGTCATTCCTACACC (reverse); HSPA5 (BiP), CAACCAACTGTTACAATCAAGGTC (forward) and CAAAGGTGACTTCAATCTGTGG (reverse); calreticulin, CGCTGCCGGAGGGTCGTTTT (forward) and GGGAAGTCCACCCGTCTCCGT (reverse); β_2-microglobulin (B2M), TTCTGGCCTGGAGGCTATC (forward) and TCAGGAAATTTGACTTTCCATTC (reverse); THPO, TGCTGTGGACTTTAGCTTGG (forward) and CTGCTCCCAGAATGTCCTGT (reverse); vascular endothelial growth factor A, CCTTGCTGCTCTACCTCCAC (forward) and CCACTTCGTGATGATTCTGC (reverse); 18 S rRNA, CACGGGAAACCTCACCCGGC (forward) and CGGGTGGCTGAACGCCACTT (reverse).

The data were analyzed by the $\Delta\Delta Ct$ method using the Alien RNA as a normalizer and the calculated values for individual mRNAs normalized to fractional enrichment (0–1) values representing the relative enrichment of a given mRNA in a given fraction. Except for 18 S rRNA, all primers were designed to be intron-spanning using the Primer3-based ProbeFinder software (Roche Applied Science).

Oligonucleotide Microarray and Data Analysis—RNA integrity was first determined with the Agilent Bioanalyzer (Agilent Technologies); all samples analyzed had RNA integrity number values of >9. Total RNA was processed for oligonucleotide microarray analysis using a Whole Transcriptome amplification kit (Agilent Technologies), and cDNAs were hybridized to GeneChip Human Gene 1.0 ST Arrays (Affymetrix). Microarray data were processed using the Genomics Suite™ software (Partek Inc.) package, and $\log_2$-transformed intensity values were exported after background correction by GC-RMA, probe summarization by Tukey's biweight median method, and no normalization. The minimum intensity cut-off value was set at

the lower quartile of the data set, and the intensity values for genes represented by multiple probe sets were averaged.

Gene Categorization—Genes were categorized into cytosolic/nuclear (cytosolic, nucleoplasmic, and mitochondrial proteins), endomembrane-resident (ER, lysosome, Golgi, endosomal, or nuclear envelope membrane-resident), or secretory pathway cargo (secretory and membrane proteins) based on the subcellular location GO categories assigned by Uniprot. The assignments were then manually verified using the following sequence features: signal peptide (predicted by SignalP), transmembrane domain (predicted by TMHMM), and mitochondrial transit peptide (predicted using TargetP), and entries with ambiguous assignments were removed from further analyses. Membrane proteins with a C-terminal anchor were removed from both endomembrane-resident and cargo categories because their targeting to the ER is post-translational.

Protein, mRNA, and Lipid Imaging—Immunoblot analyses were performed as described previously (28–30). Single molecule mRNA imaging was performed with Stellaris FISH probes (Cell Search Technologies) as per the manufacturer's protocols. ER membrane integrity was imaged with ER-Tracker Blue-White DPX (Invitrogen). Ceramide imaging was performed using BODIPY FL C5-ceramide (Invitrogen) as per the manufacturer's instructions.

Fluorescence Imaging and Analysis—All imaging was performed on a Deltavision Elite deconvolution microscope (Applied Precision) equipped with ×100, numerical aperture 1.4 oil immersion objective (UPlanSApo 100XO; Olympus) and a high resolution CCD camera (CoolSNAP HQ2; Photometrics). Images were acquired as *Z*-stacks at 0.2-μm intervals at identical exposure settings across all samples for a given imaged protein, RNA, or lipid. Image data were deconvolved using the SoftWoRx program (Applied Precision) and processed on ImageJ/FIJI and Adobe Photoshop (Adobe Systems) to render maximum intensity projections, merge channels, and pseudocolor images. Adjustments in image brightness/contrast were limited to linear changes and were applied uniformly across all images in a given experiment. The number of RNA molecules/cell was measured using the spot-counting module of the Imaris version 7.3 software (Bitplane) with automated thresholding. The mean number of RNA spots/cell was calculated for 10–45 cells in each sample and plotted using GraphPad Prism, with *error bars* representing S.E. The final figures were assembled on Adobe Illustrator version 15.1.0 (Adobe Systems).

RNA Cross-linking to Endoplasmic Reticulum Membrane Proteins—Canine rough microsomes (RM) were irradiated with 264-nm UV light (Stratagene Stratalinker) for 30 min on ice and nuclease-digested, and the RNA was ^{32}P-labeled, as described below, following purification of the membrane protein fraction by either alkali extraction or Triton X-114 cloud point partitioning (33, 34).

RNA-dependent T4 RNA Ligase Labeling of UV-irradiated RM—RM-associated RNAs were digested with mung bean nuclease at a final concentration of 1 unit/μg RNA and incubated at 30 °C for 1 h. RM were collected by ultracentrifugation, and the RM pellet was resuspended in lysis buffer. For T4 RNA ligase reaction, the RM fractions were adjusted to a final concentration of 50 mM Tris-HCl, pH 7.5, 10 mM $MgCl_2$, 1 mM DTT, 15% DMSO, 1 mM ATP, 80 μCi of [5′-^{32}P]cytidine 3′,5′-bis(phosphate), 1 unit/μl T4 RNA ligase (New England Biolabs), and incubated at 4 °C. The lysate was collected, TCA-precipitated, and analyzed by SDS-PAGE and phosphorimaging.

Proteomic Analysis of HeLa Polysomes—HeLa cell cultures were fractionated as described above, and polyribosomes from the cytosol, Brij-sensitive ER, and Brij-resistant ER fractions were purified by sucrose density gradient centrifugation. The polyribosome fractions were concentrated by ultracentrifugation, and 30 μg of each sample was concentration-normalized to ~0.1 μg/μl with 50 mM ammonium bicarbonate (AmBic) and then supplemented with Rapigest SF surfactant (Waters) to a final concentration of 0.1% (w/v). Cysteine reduction (10 mM DTT), alkylation (20 mM iodoacetamide), and trypsin digestion was then performed. After digestion, all samples were supplemented with 33 fmol of ADH1_YEAST digest (Massprep standard, Waters Corp.)/μg of total protein as a surrogate standard, acidified to 1% TFA, and heated to 60 °C for 2 h to hydrolyze Rapigest surfactant. Finally, the samples were taken to dryness in a SpeedVac (Eppendorf) and resuspended in 100 mM ammonium formate (pH 10) at a concentration of 1.0 μg/μl prior to analysis. Quantitative two-dimensional liquid chromatography-tandem mass spectrometry (LC/LC-MS/MS) was performed on 3 μg of protein digest/sample, and each sample was analyzed twice, once in ion mobility MS mode (HDMS^E) for simultaneous qualitative/quantitative analysis and once by data-dependent acquisition (DDA) mode for supplementary peptide identifications (35–37). Following all analyses, data were imported into Rosetta Elucidator version 3.3 (Rosetta Biosoftware, Inc.), and all LC/LC-MS runs were aligned based on the accurate mass and retention time of detected ions ("features") using the PeakTeller algorithm (Elucidator). The peptide abundance was calculated based on the area under the curve of aligned features across all runs. The MS/MS data were searched against a SwissProt database with human taxonomy, which also contained a reversed sequence "decoy" database for false positive rate determination. Database searching for HDMS^E data were performed in PLGS version 2.5 and for DDA data using Mascot version 2.2. Database searches were combined within the Elucidator software package, and aggregate scoring was performed using the PeptideProphet algorithm. The data were annotated at a PeptideProphet score of 0.73, resulting in a 0.7% peptide false discovery rate (38, 39). To allow relative molar composition comparisons for the different components making up the polyribosome fractions, we used the "Best Flier" method of Silva *et al.* with minor modifications, as described previously (40–42).

Proteomic Analysis of Canine Rough Microsome-associated mRNPs—Canine pancreas rough microsomes were detergent-solubilized, and the polysome fraction was obtained by sucrose gradient velocity sedimentation. Polysome fractions were pooled and concentrated by ultracentrifugation. Polysome pellets were then gently resuspended, and a binding control fraction was prepared by digestion of one-half of the sample with staphylococcal nuclease. Following the addition of 15 mM EDTA to all samples, to dissociate the ribosomal subunits and release mRNPs, poly(A) mRNPs were selected on Oligo(dT)-

Cellulose Type 7 resin (GE Healthcare). Following extensive washing in EDTA-supplemented buffers, poly(A) mRNA-associated proteins were released by the addition of 10 mM AmBic, 15% dimthylformamide. Eluted proteins were concentrated by TCA precipitation and separated on 4–12% Bis-Tris gradient gels (Life Technologies), and in-gel digestion was performed as described (43). Approximately one-half of each digest (5 μl) was fractionated on a C18 column (Waters) using a gradient of 5–40% acetonitrile with 0.1% formic acid on a nanoAcquity liquid chromatograph (Waters). Electrospray ionization was used to introduce the sample in real-time to a Q-Tof Synapt G1 mass spectrometer (Waters), collecting data for each sample in DDA mode. Raw data were processed in Mascot Distiller (version 2.3) and searched in Mascot version 2.2 (Matrix Science) against the NCBInr database with mammalian taxonomy. Scaffold (version 3.6.2; Proteome Software Inc.) was used to validate MS/MS-based peptide and protein identifications. Measured peptide and protein level false discovery rate were both determined to be 0.0% using the target-decoy strategy.

For photocross-linking studies, RM were UV-irradiated in a Stratalinker 24000 at 0.8 J/cm^2 for four cycles on ice. Samples were adjusted to a final concentration of 0.5 M KOAc, 15 mM EDTA, 50 units/ml RNaseOUT, protease inhibitor mixture and incubated for 30 min on ice. KOAc/EDTA-washed RM were collected by ultracentrifugation and resuspended in a oligo(dT) resin equilibrium buffer (0.5% LiDS, 0.5 M LiCl, 10 mM Tris-HCl, pH 7.2, 5 mM DTT, 15 mM EDTA), heated to 65 °C for 5 min, and cooled on ice. The solubilized RM suspension was then centrifuged to remove detergent-insoluble materials, and the supernatant was chromatographed on Oligo(dT)-Cellulose Type 7 resin (GE Healthcare). Unbound material was removed by extensive washing in oligo(dT) resin equilibrium buffer, and the RNA-associated RBPs were subsequently eluted by the addition of a buffer consisting of 10 mM Tris-HCl, pH 7.2, 1 mM EDTA, 0.1% Triton X-110 with 1:50 (v/v) RNase A/T1 Mix (Thermo Scientific) at room temperature for 30 min. Eluted proteins were concentrated by TCA precipitation, and their composition was assessed by immunoblot.

RESULTS

Divergent Modes of Ribosome-mRNA Association with the ER Membrane—In cell-free translation/translocation systems, mRNAs are co-translationally localized to the ER and anchored indirectly via ribosome binding to the protein-conducting channel (3, 8, 44). In contrast, analyses of *in situ* mRNA-ER interactions conducted with rough microsomes (RM) have demonstrated that ER-associated mRNAs can be binned into two broad classes: those that are bound via ribosome-dependent (indirect) and those that undergo ribosome-independent (direct) ER-mRNA anchoring (Fig. 1*A*) (13, 15, 45–47). These differences are significant because they suggest that mRNA localization and anchoring to the ER is selective and regulated and so may contribute significantly to gene expression.

To better understand mechanisms of ER-mRNA association, we developed methods to study mRNA-ER interactions in semi-intact cells, whose ER morphology and function more closely approximate the *in vivo* scenario and where cytosolic and ER-associated mRNAs can be reliably separated (48). Our experimental approach is schematically illustrated in Fig. 1*A*. First, tissue culture cells are permeabilized with a digitonin-supplemented cytosol buffer to permeabilize the plasma membrane and release the cytoplasmic mRNA pool (28, 49). The digitonin-permeabilized (semi-intact) cells are then treated with salts, chelating agents, and/or detergents, and mRNA-ER interactions were assessed by examining the mRNA composition of the released and ER-associated fractions (13, 15, 45–47). Using HeLa cells as a model, we first examined the ER association properties of two mRNAs, B2M (a secretory protein) and GRP94 (a resident protein of the ER lumen), because previous studies with RM had identified these mRNAs as undergoing either ribosome-dependent (B2M) or ribosome-independent (GRP94) membrane association (13, 15). In contrast to prior findings with RM, in semi-intact HeLa cells, B2M transcripts remained wholly membrane-bound under conditions (high salt extraction) that yielded their efficient release from RM (Fig. 1*B*). The reason for these differences is not yet known, although it has been suggested that differences in endogenous nuclease activity, tissue source, and buffer composition used during RM isolation can significantly influence the biochemical properties of RM-associated mRNAs (46, 50, 51).

Because ER morphology and polysome structure in semi-intact cells more closely approximates the *in vivo* scenario then that of RM, where polysome structure is frequently compromised, we postulated that mRNA-ER interactions in semi-intact cells would be more stable to biochemical extraction. We thus screened detergent/salt admixtures for their ability to solubilize mRNAs from digitonin-permeabilized HeLa cells. Intriguingly, we found that extraction with Brij35/Tris or Brij58/Tris detergent/salt admixtures revealed divergent membrane association properties for B2M and GRP94 mRNAs, where B2M mRNAs were efficiently solubilized and GRP94 mRNAs were refractory to solubilization (Fig. 1*B*). By varying the detergent component in the screen, we found that selective mRNA release correlated with detergent hydrophile-lipophile balance (HLB), with high HLB detergents (*e.g.* Brij35 (HLB = 17.0)) yielding selective mRNA release and low HLB detergents, such as Triton X-100 (HLB = 13.6) or the bile salt derivative CHAPSO, efficiently solubilizing both B2M and GRP94 mRNAs. Importantly, the combination of high salt (0.5 M Tris) and Brij detergent was synergistic; neither 0.5 M Tris nor Brij detergent alone was sufficient for selective mRNA release (Fig. 1*B*). These findings were not unique to the B2M- and GRP94-encoding mRNAs; mRNAs encoding the secretory proteins B2M, vascular endothelial growth factor A, and thrombopoietin were efficiently solubilized in Tris/Brij35 buffers, whereas mRNAs encoding the ER-resident proteins GRP94, BiP, and calreticulin were refractory to Tris/Brij35 solubilization (Fig. 1*C*), suggesting that mRNAs undergo cohort-specific binding interactions with the ER.

Although we assayed mRNA release in the salt/detergent screen above, the mRNAs are ER-bound as polysomes, so the divergent solubilization behaviors could simply arise from differences in nascent polypeptide chains (*e.g.* signal sequence functionality, interactions with the protein translocation machinery), differences in ribosome loading and/or open reading frame size, and/or mRNA-specific binding interactions

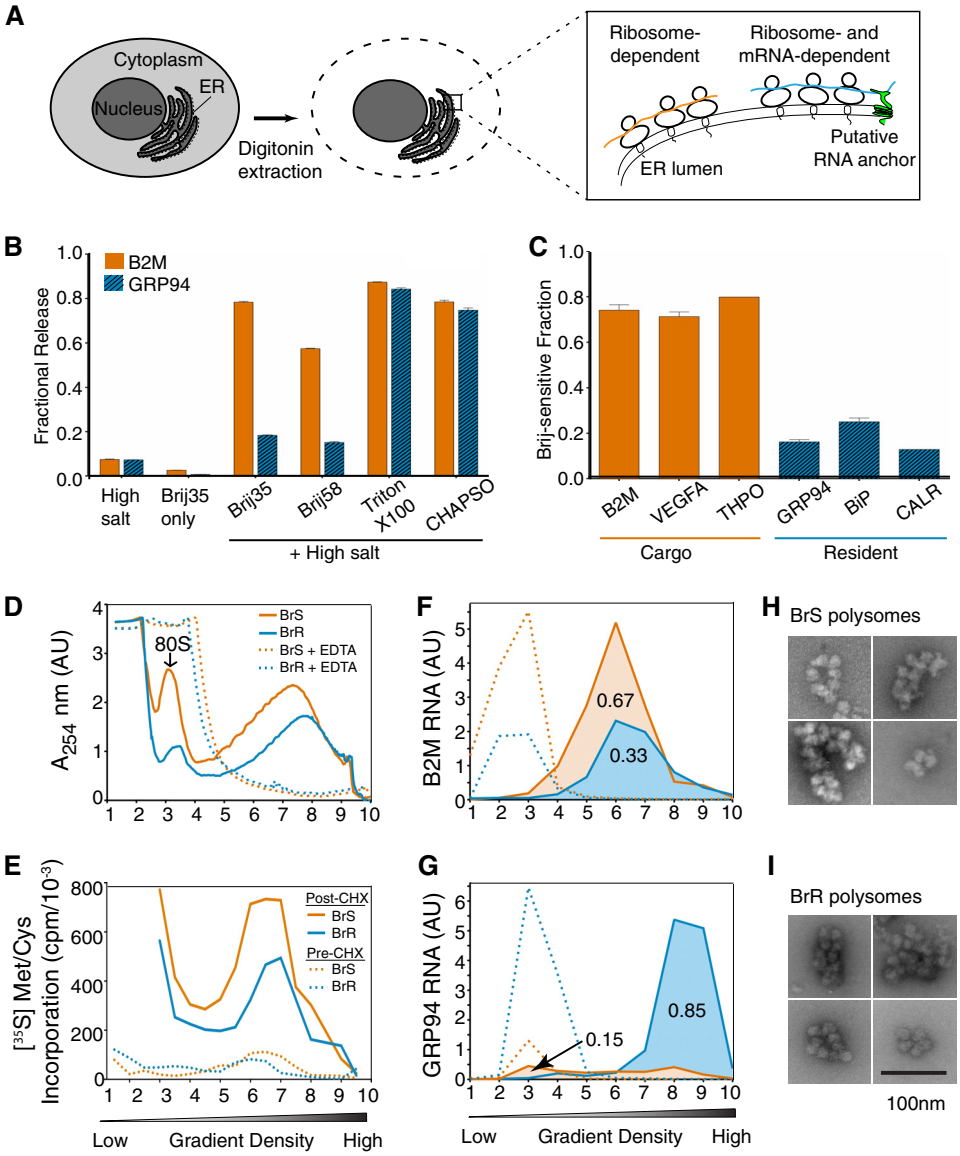

FIGURE 1. **Endoplasmic reticulum-associated mRNAs are partitioned between detergent-resistant and detergent-sensitive membrane domains.** *A*, schematic of experimental system used to assess ER-ribosome/mRNA interactions in tissue culture cells. *B*, 0.5 M Tris, Brij35, or admixtures of Tris and Brij35, Brij58, Triton X-100, or CHAPSO were screened for their capacity to solubilize mRNAs encoding GRP94 (*yellow*) or B2M (*blue*). mRNA levels were determined by qRT-PCR and normalized to fractional distribution values. *C*, the distributions of mRNAs encoding B2M, vascular endothelial growth factor A (*VEGFA*), and thrombopoietin (*THPO*) (*yellow bars*), and the ER proteins GRP94, BiP, and calreticulin (*blue bars*) in the Brij35-sensitive fraction of HeLa cells were determined by qRT-PCR. Data depicted in *B* are an average of three independent experiments, and data in *C* are an average of six independent experiments. *Error bars*, S.E. *D*, polysomes from the BrS and the BrR fractions were analyzed by sucrose gradient velocity sedimentation in the absence and presence of EDTA. *E*, translation activity of BrS and BrR polysomes; HeLa cells were labeled with [^{35}S]Met/Cys in the presence or absence of cycloheximide and fractionated as in *D*, and the ribosome-associated polypeptides in the gradient fractions were quantified by liquid scintillation counting of the TCA-precipitated proteins. *F* and *G*, the distributions of B2M (*F*) and GRP94 (*G*) mRNAs in BrS- and BrR-derived polysome fractions in the absence (*solid lines*) or presence (*dotted lines*) of EDTA. *H* and *I*, negative staining electron microscopy images of polysomes derived from the BrS (*H*) and BrR (*I*) fractions. *Bar*, 100 nm. *AU*, relative absorbance units. *Error bars*, S.E.

with components of the ER membrane, any or all of which could alter binding interactions and/or avidity. However, by accepted criteria (mean length, hydrophobicity score), the signal peptides of the two cohorts of mRNAs were quite similar (Table 1). In addition, comparisons of open reading frame and overall transcript length did not distinguish the two; thrombopoietin (36 kDa), for example, is encoded by an 1805-bp mRNA, whereas calreticulin (48 kDa) is encoded by a 1929-bp mRNA, yet the two mRNAs display divergent modes of membrane association (Table 1). To address possible differences in translation/ribosome loading, we examined the translational status of the polysomes recovered in the Brij-sensitive (BrS) and Brij-resistant (BrR) fractions. When analyzed by sucrose density gradient centrifugation, the polysome profiles of the two fractions were quite similar (Fig. 1*D*), a conclusion that we confirmed by examining the EDTA sensitivity of the ribosome profiles and by negative staining electron microscopy imaging of the polysome fractions (Fig. 1, *D*, *H*, and *I*) (52). In addition, both polysome pools were translationally active; analysis of gradient fractions obtained from [^{35}S]Met/Cys-labeled cells demonstrated a high degree of overlap in the ribosome and radio labeled nascent polypeptide chain profiles (Fig. 1, *D* and *E*).

TABLE 1
Characteristics of proxy secretory and endomembrane protein-encoding mRNAs and their encoded proteins

Category	Gene	Protein product	Intracellular location	mRNA properties (length)			Signal properties[a]		
				5′-UTR	CDS	3′-UTR	SS	TM	HS
					nt				
Cargo	B2M	β_2-Microglobulin	Secreted	60	360	567	Yes	No	1.581
	VEGFA	Vascular endothelial growth factor A	Secreted	498	1239	1940	Yes	No	0.585
	THPO	Thrombopoietin	Secreted	215	1062	528	Yes	No	1.5
Endo	GRP94/HSP90B1	Heat shock protein 90 kDa β	ER lumen	105	2412	263	Yes	No	1.327
	BiP/HSPA5	Heat shock 70-kDa protein 5	ER lumen	261	1965	1747	Yes	No	1.384
	CALR	Calreticulin	ER lumen	80	1254	595	Yes	No	2.089

[a] Signal properties are as follows. SS, signal sequence; TM, transmembrane domain; HS, hydrophobicity score (average hydrophobicity score of the signal peptide calculated using Kyte-Doolittle amino acid hydrophobicity scores).

These findings were further validated in experiments where cycloheximide was added prior to the addition of radiolabeled amino acids. Under these conditions, ^{35}S incorporation was reduced by >95%, with the remaining fraction probably representing ribosome-associated [^{35}S]Met/Cys aminoacyl tRNAs. Last, the B2M (~350-bp) and GRP94 (~2300-bp) mRNAs were enriched in the BrS and BrR polysome fractions in the absence but not the presence of EDTA (Fig. 1, *F* and *G*). Combined, these data are consistent with the view that polysomes are bound to the ER by multiple mechanisms and suggest that for the endomembrane-resident mRNAs, the mRNA itself contributes to the binding interactions. Relevant to this point, prior studies have demonstrated that native ribosome-Sec61 interactions are quite salt-resistant, with only partial disruption reported at salt concentrations as high as 1.2 M (53). It would appear, then, that the polysomes recovered in the BrS fraction are bound to sites other than Sec61 and/or are bound to Sec61 in a manner distinct from the salt-resistant Sec61 binding behavior of the BrR polysomes.

ER-associated mRNAs Are Partitioned between Detergent-induced Sphingolipid-rich and Spingolipid-poor ER Membrane Domains—That ER-associated mRNAs displayed distinct Brij solubilization profiles was of great interest because Brij detergents are well known to display selective membrane solubilization behavior, where they efficiently solubilize glycerophospholipids but are ineffective in solubilizing sphingolipids and subsets of integral membrane proteins (54, 55). Although these findings have been interpreted as evidence for membrane microdomains, in the context of this study, we considered that Brij detergents could serve as useful biochemical tools for identifying candidate ribosome- and/or mRNA-interacting proteins in the BrS and BrR fractions.

As a means of validating this approach, we examined ER-associated mRNAs and ER membrane structure in HeLa cells fractionated by the three-detergent sequence noted above. In these experiments, mRNAs were individually imaged by single molecule RNA FISH (56), and ER membrane components were imaged by ER-selective membrane and protein reagents. Representative micrographs depicting B2M and GRP94 mRNA distributions through the sequential detergent extraction protocol are shown in Fig. 2*A*, with quantification data included as *insets*. Similar to the data reported in Fig. 1*B*, extraction of digitonin-permeabilized HeLa cells with the Brij/Tris buffer resulted in the release of ~75% of ER-associated B2M mRNAs but only ~10% of GRP94 mRNAs. Following extraction with dodecylmaltoside, GRP94 mRNAs and the remaining small fraction of Brij35-resistant B2M mRNAs were released. These data demonstrate, by an orthogonal approach, mRNA-selective modes of polysome association with the ER.

To assess the effects of sequential detergent extraction on ER membrane structure, we first visualized the ER network with ER-Tracker Blue-White DPX (Fig. 2*B*). Here, the ER-Tracker Blue-White DPX staining patterns of intact and digitonin-treated cells were nearly identical, although overall intensities were diminished following digitonin treatment. We attribute the decrease in fluorescence intensity to a partial redistribution of ER-bound probe into the detergent-supplemented buffers. Subsequent treatment with Tris/Brij35 resulted in the complete loss of ER-Tracker Blue-White DPX staining, indicative of a loss of ER membrane integrity. This conclusion was further supported by immunostaining for the ER lumenal protein GRP94, which was distributed throughout the ER of unfractionated and digitonin-treated cells and absent following Tris/Brij35 extraction (Fig. 2*C*). Given the lipid selectivity of Brij detergents, we also examined HeLa ER sphingolipid distributions in experiments where HeLa cells were biosynthetically labeled with BODIPY FL C5-ceramide and subsequently fractionated (Fig. 2*D*). BODIPY FL C5-ceramide undergoes concentration-dependent excimer formation that serves as a convenient marker of subcellular (*e.g.* Golgi) ceramide enrichment (57, 58). Following short (5-min) labeling periods, the ER displayed diffuse BODIPY-ceramide fluorescence (*green*) with a perinuclear Golgi enrichment (*red*) (57, 58) (Fig. 2*D*). This staining pattern was enhanced following digitonin treatment, and BODIPY-ceramide excimer clusters were prominent in the Golgi (Fig. 2*D*). Following Tris/Brij35 extraction, however, BODIPY-ceramide distributions were dramatically altered, with Golgi structures no longer discernible and the BODIPY-ceramide present throughout the ER (*green channel*) and as numerous sphingolipid-dense clusters (*red channel*) (Fig. 2*D*). Subsequent extraction with dodecylmaltoside yielded a nearly complete loss of BODIPY-ceramide staining. These data provide a clear illustration of the lipid selectivity of Brij35 extraction (54) and allowed us to determine whether GRP94 mRNAs were enriched in the Brij-induced ceramide clusters. Co-localization studies were thus performed where GRP94 single molecule RNA FISH was performed on BODIPY-ceramide-labeled HeLa cells (Fig. 2*E*). As depicted, GRP94 mRNAs were largely if not entirely resolved from the ceramide clusters, although they were retained in the ceramide-rich ER remaining after Brij extraction. Combined, these data provide a morphological correlate to the data depicted in Fig. 1 and demonstrate a hetero-

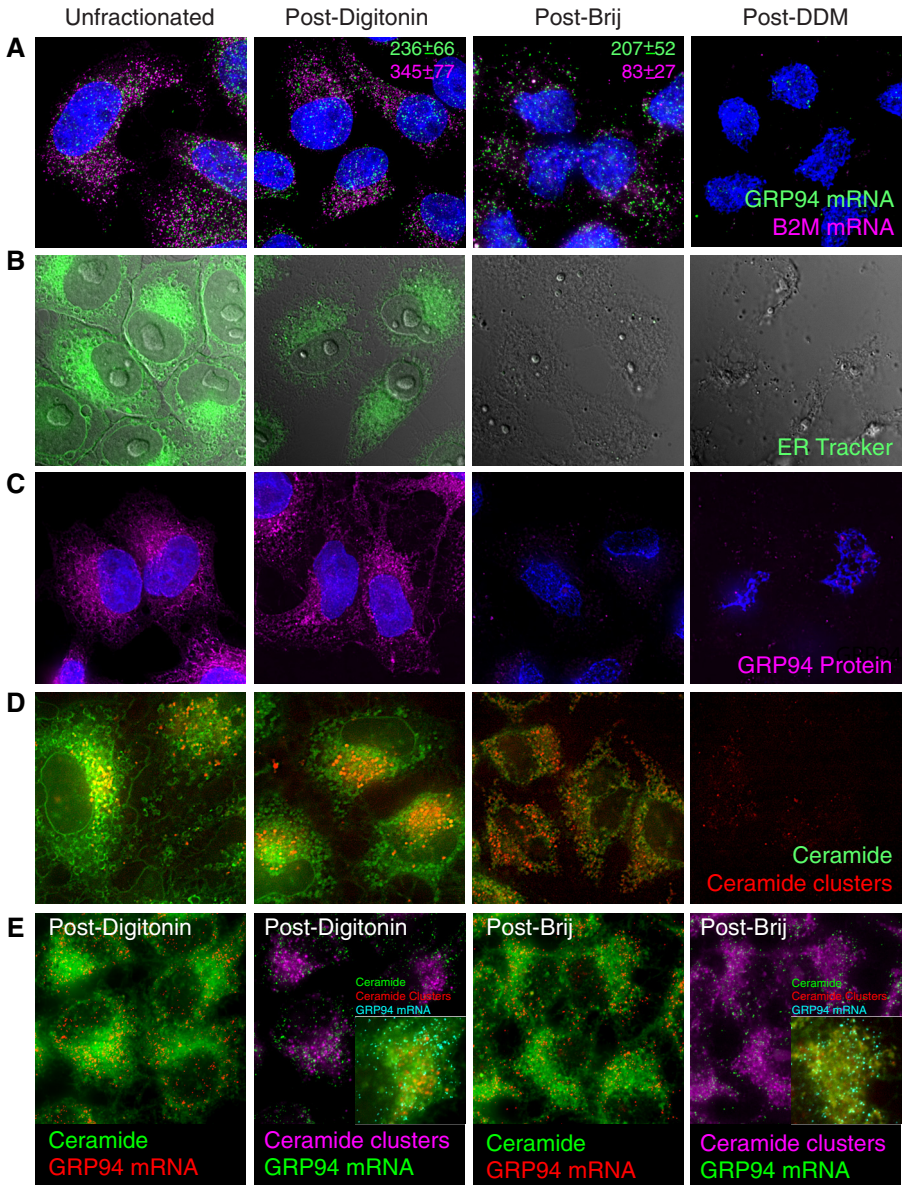

FIGURE 2. **Analysis of ER morphology and mRNA distributions in detergent-fractionated HeLa cells.** HeLa cell cultures were either untreated (*Unfractionated*), extracted with digitonin-supplemented cytosol buffer (*Post-Digitonin*), sequentially extracted with digitonin-supplemented cytosol buffer followed by Tris/Brij35 (*Post-Brij*), or subjected to the identical series of treatments, followed by extraction with dodecylmaltoside-supplemented buffers (*Post-DDM*). *A*, HeLa cells were fixed directly (*Unfractionated*) or following sequential detergent extraction and stained for B2M and GRP94 mRNAs. *Z*-Stack images were acquired on a DeltaVision microscope, and deconvolved, maximum intensity projected micrographs are depicted. *Inset*, normalized quantification of RNA counts. Spot counting was performed using the Bitplane Imaris software and default threshold settings. The total number of mRNAs/cell was determined for 10–45 cells, and mean ± S.E. values are depicted. *B*, cells were biosynthetically labeled with ER-Tracker Blue-White DPX and fractionated as described above. *C*, cells were fractionated as described above and stained for the ER lumenal protein GRP94. *D*, cell cultures were biosynthetically labeled with BODIPY FL C5-ceramide and fractionated as described above. *E*, HeLa cell cultures were biosynthetically labeled with BODIPY FL C5-ceramide, followed by single molecule fluorescence imaging of GRP94 and B2M mRNAs as described above.

geneous ER, where different mRNAs are anchored to membrane components that themselves can be distinguished by their detergent-sensitive partitioning to sphingolipid-rich ER membrane domains.

Divergent Modes of ER-mRNA Association Are Characteristic of the ER-mRNA Transcriptome—To determine whether the differing modes of mRNA-ER interaction described above reflected an mRNA transcriptome-wide organization of mRNA anchoring to the ER, we next determined the mRNA compositions of the BrS and BrR fractions by oligonucleotide microarray (Fig. 3 and supplemental Table S1). A histogram depicting mRNA enrichment in the BrR fraction is shown in Fig. 3*A* and, interestingly, details a tailed, non-normal distribution. By fitting a two-component mixture model to these data (Fig. 3*B*), we identified a major population of mRNAs with a median BrR distribution of 0.38 and a second, smaller population of mRNAs with a highly significant enrichment in the BrR fraction (median = 0.65). The mRNA distribution data determined by oligonucleotide microarray revealed that endomembrane-resident protein-encoding transcripts were highly enriched in the BrR fraction. We thus analyzed the data set in a three-category model where ER-associated mRNAs were sorted as either cyto-

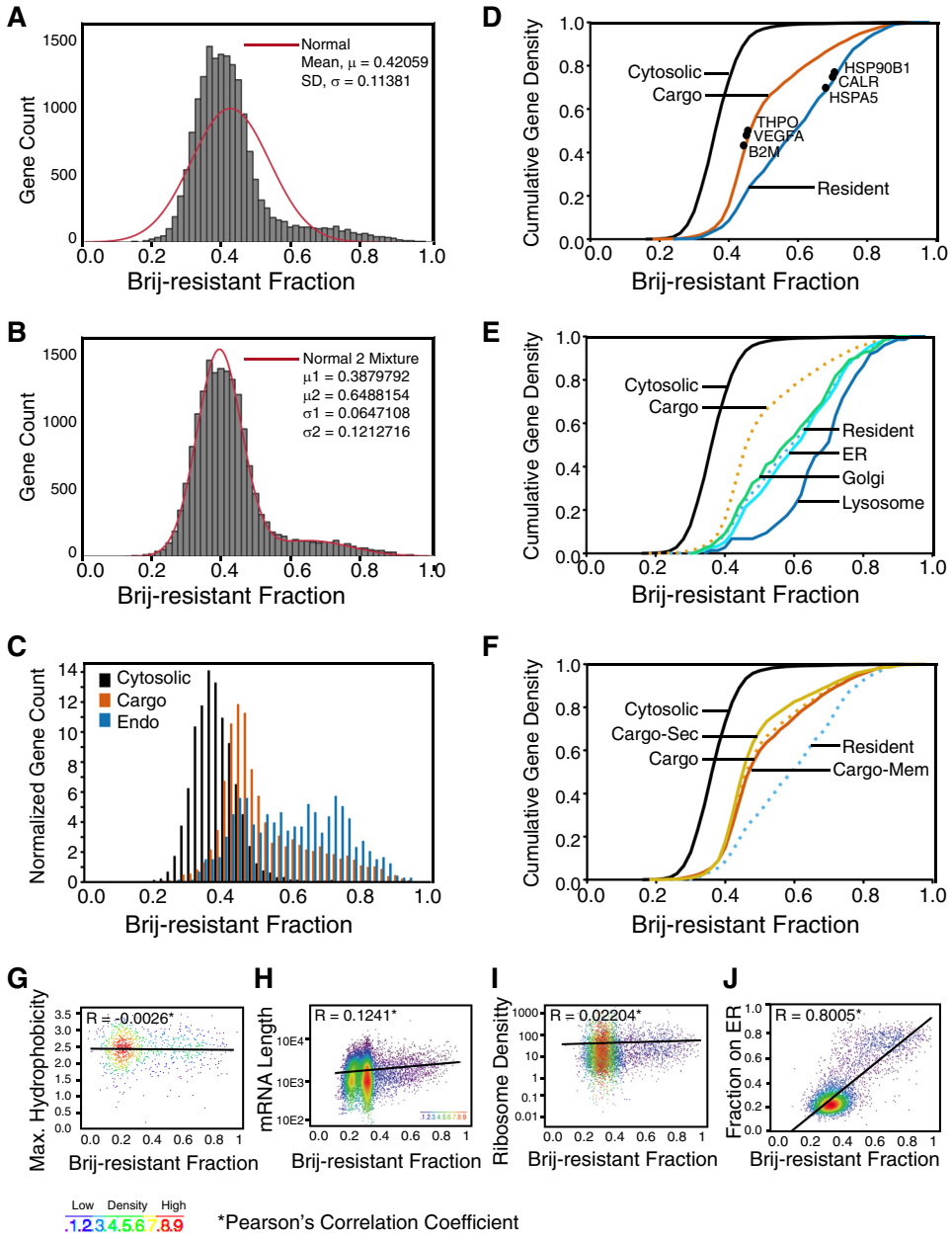

FIGURE 3. **cDNA microarray analysis of mRNA partitioning to the Brij35-resistant fraction of HeLa ER.** *A* and *B*, mixture modeling of mRNA enrichments in the Brij-resistant fraction. In *A*, the *red line* depicts a normal distribution; in *B*, the *red line* depicts a tailed, two-component distribution. *C*, relative distributions of the three primary cohorts of mRNAs, those encoding cytosolic proteins (*Cytosolic*), secretory pathway cargo proteins (*Cargo*), or endomembrane resident proteins (*Endo*). *D*, cumulative gene density distributions of the data presented in *C*. Shown are the three primary mRNA categories noted in *A* with the distributions of the six mRNAs analyzed in Fig. 1*C* denoted, demonstrating the concordance between the qRT-PCR and cDNA microarray data sets. *E*, CGD distributions of the components of the endomembrane-resident gene category. *F*, CGD distribution of the mRNA cohort encoding soluble secretory (*Cargo-Sec*) and membrane proteins (*Cargo-Mem*). *G–J*, analyses of gene distribution in the Brij35-resistant fraction as a function of encoded signal sequence hydrophobicity (*G*), mRNA length (*H*), ribosome loading density (*I*), or enrichment on the ER (*J*). Pearson's correlation coefficients are included as *insets* for each analysis.

solic ($mRNA_{cyt}$), secretory pathway cargo ($mRNA_{cargo}$), or endomembrane-resident ($mRNA_{endo}$). Histograms depicting the fractional BrR enrichment for each category were plotted as a function of normalized gene count (Fig. 3*C*). $mRNA_{cyt}$ were the most numerous ($n = 6687$) and displayed the lowest BrR enrichment values (median = 0.32). $mRNA_{cargo}$ ($n = 2931$) displayed a median BrR enrichment of 0.44, and $mRNA_{endo}$ ($n = 734$) displayed a median BrR enrichment of 0.59. These differences are further illustrated in a cumulative gene density plot (Fig. 3*D*), where the qRT-PCR-determined BrR partitioning values for the genes examined in Fig. 1*C* are also indicated and demonstrate both the divergent membrane association properties of the ER-associated transcripts and a strong correlation between the mRNA partitioning values determined by oligonucleotide microarray and qRT-PCR (*solid circles*). Statistical analysis of these data by the Kolmogorov-Smirnov test indicated that the differences in the BrR distributions of the three gene categories were highly significant ($p < 10^{-16}$; Table 2).

In further analyses, organelle-specific subcategories of $mRNA_{endo}$ were defined, and their cumulative density distributions in the BrR fraction were plotted (Fig. 3*E*). Unexpectedly, an organelle-specific grouping revealed that mRNAs encoding

TABLE 2

Two-sample Kolmogorov-Smirnov test results for pairwise comparisons of mRNA cohorts, calculated using the R statistical package

The distance statistic indicates the population deviation, and the associated *p* value indicates the population deviation probability. Populations exhibiting significant differences are indicated in boldface type.

Population 1	Population 2	Distance (D)	*p* value
Cytosolic	**Cargo**	**0.5754**	**2.20E-16**
Cytosolic	**Endo**	**0.674**	**2.20E-16**
Cargo	**Endo**	**0.2824**	**2.20E-16**
Endo	ER	0.0856	5.79E-02
Endo	Golgi	0.0474	9.19E-01
Endo	**Lyso**	**0.3375**	**4.27E-07**
Cargo	Mem	0.0369	9.11E-02
Cargo	Sec	0.0905	3.05E-04

lysosome-resident proteins were remarkably BrR-enriched and distinct from the ER- and Golgi-resident protein mRNAs, perhaps suggestive of a function for the ER in "prelysosomal" biogenesis, as has been reported for preperoxisome biogenesis (59) (Fig. 3*E* and supplemental Table S1). In the secretory pathway cargo cohort, we also compared the distribution of mRNAs encoding plasma membrane (Fig. 3*F*, *Cargo-Mem*) and secreted proteins (*Cargo-Sec*). Neither class of mRNAs deviated significantly from the total cargo population (*Cargo*), indicating that encoded topogenic signals (*e.g.* signal peptide, transmembrane domain) are not primary determinants of mRNA partitioning to the BrS or BrR fractions (Fig. 3*F*). In addition, for those genes encoding signal sequences, there was no correlation between the calculated signal peptide hydrophobicity and mRNA enrichment in the BrR fraction (Fig. 3*G*).

We also determined whether open reading frame length or ribosome loading, both of which could contribute to the avidity of mRNA/polysome association with the ER, correlated with mRNA partitioning to the BrR fraction. As shown in Fig. 3, *H* and *I*, neither mRNA length nor ribosome loading density (number of ribosomes/mRNA) (12) correlated with the ER membrane association properties of the mRNA. In contrast, when mRNA enrichment in the BrR fraction was plotted as a function of the fractional distribution to the ER (determined in Ref. 12), a strong correlation was observed (Fig. 3*J*) (*i.e.* mRNAs displaying the strongest localization to the ER also display the highest anchoring to the BrR-ER, and *vice versa*). These data highlight the distinctive molecular signature of the endomembrane-resident protein-encoding mRNAs and raise the important question of their mechanism of association with the ER membrane (12, 13, 15).

Identification of RNA-binding ER Membrane Proteins—Past and recent studies have provided evidence for the direct (ribosome-independent) association of endomembrane mRNAs with the ER (10, 12–16). Given the detergent solubilization properties of the endomembrane mRNAs reported above, we considered that this mRNA cohort might directly bind to resident integral membrane RBPs, although it is equally plausible that mRNA anchoring could occur via binding interactions between soluble RBPs and cognate ER RBP binding proteins. To date, no resident ER integral membrane proteins containing canonical RNA binding domains have been identified. Recent proteomic screens have revealed, however, a surprising diversity of proteins with RNA binding activity, many of which lack known RNA binding domains and/or whose RNA binding activity remains to be characterized (60–63). Consistent with these findings, mRNA binding activity has been proposed for one resident ER membrane protein, p180 (RRBP1) (14).

As a relatively unbiased approach to the question of indirect or direct RNA anchoring to the ER, we screened for integral ER-RNA-binding proteins by UV cross-linking, a "zero-length" protein-nucleic acid cross-linking method (60, 64). To focus the analysis on ER integral membrane proteins, experiments were performed with canine pancreas RM, a highly enriched ER membrane preparation that is virtually devoid of other contaminating organelle membranes (65). The experimental protocol used is illustrated in Fig. 4*A*. Here, RM were UV-irradiated to generate protein-RNA cross-links, peripheral proteins were released by salt/EDTA or mild alkali extraction (34), and the "stripped" RM were collected by ultracentrifugation. The irradiated, stripped RM were then digested with mung bean nuclease to generate protein-RNA adducts bearing free 3′-OH groups, which were then selectively labeled using T4 RNA ligase/[^{32}P]cytidine 3′-5′bisphosphate (66). In contrast to alkaline extraction, which releases both peripheral and lumenal proteins, the salt/EDTA-washed RM contain substantial quantities of lumenal proteins and therefore were subjected to multiple rounds of Triton X-114 partitioning to isolate the ER integral membrane protein fraction, which is enriched in the detergent phase and is readily distinguished from the fraction of soluble proteins, which is enriched in the aqueous phase (33, 67). Shown in Fig. 4*B* are Coomassie Blue-stained SDS-polyacrylamide gels of the two ER membrane protein fractions (alkali-extracted and Triton X-114-selected), where gels were loaded as either membrane equivalents, to illustrate the high relative abundance of ribosomal and lumenal *versus* integral membrane proteins, or protein equivalents, to more clearly reveal the ER integral membrane protein proteome. Immunoblots for the lumenal proteins GRP94 and BiP and the membrane proteins ribophorin I, Sec61α, and TRAPα demonstrate that the two procedures effectively separate soluble and integral membrane proteins (Fig. 4*C*). Importantly, these data demonstrate that the integral membrane protein fractions (detergent phase for the Triton X-114 extraction and P for the alkali extraction) lack "false positives"; the soluble proteins BiP and GRP94 were entirely absent from the integral membrane protein fractions.

The results of the [^{32}P]pCp/T4 RNA ligase labeling experiments are depicted in Fig. 4*D* and demonstrate that the labeling reaction was strictly T4 RNA ligase-dependent (Fig. 4*D*, *lane 1 versus lane 2*) and yielded numerous radiolabeled protein-RNA adducts of apparent molecular masses ranging from 15 to 70 kDa in the ER integral membrane protein fractions obtained via Triton X-114 partitioning (detergent phase) or alkali extraction (*Alkali*) (Fig. 4*D*, *lanes 3* and *4*, respectively). These data demonstrate that numerous ER membrane proteins display direct RNA binding activity. Because this protocol for detecting RNA binding activity does not distinguish between mRNA, rRNA, tRNA, and/or non-translated RNAs, complementary approaches were developed to identify the ER membrane proteins functioning in mRNA anchoring (68–70).

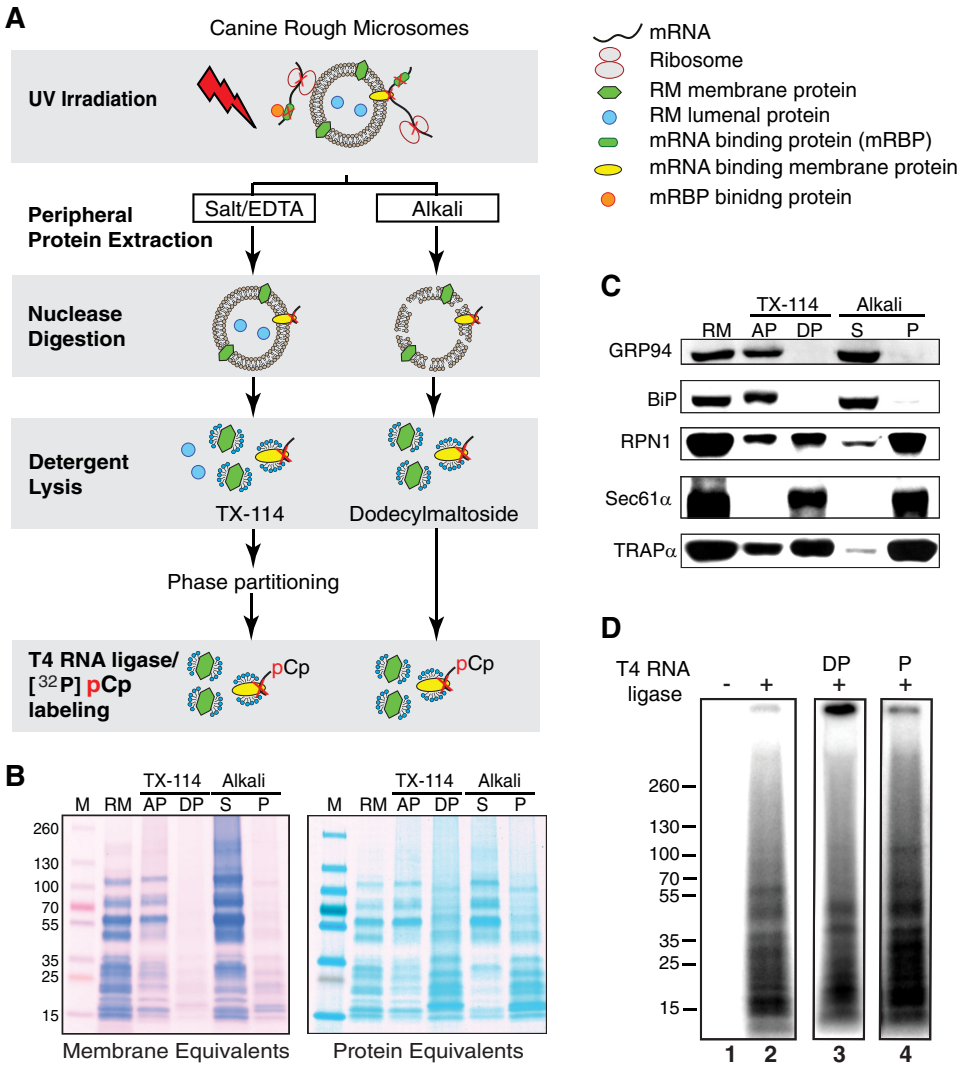

FIGURE 4. **UV-cross-linking reveals RNA-binding endoplasmic reticulum membrane proteins.** *A*, schematic of experimental protocol for the identification of ER integral membrane RNA-binding proteins. *B*, images of SDS-PAGE/Coomassie Blue-stained gels depicting the membrane protein enrichments obtained by Triton X-114 (*TX-114*) or alkali extraction, with protein loadings as membrane equivalents (derived from identical quantities of RM) or protein equivalents (identical quantities of total protein). *AP*, aqueous phase; *DP*, detergent-rich phase; *S*, alkali-releasable proteins; *P*, alkali-resistant fraction (membrane proteins). *C*, immunoblot analysis of ER lumenal proteins (GRP94, BiP) and ER membrane proteins (ribophorin I (*RPNI1*), Sec61α, or TRAPα in the aqueous or detergent-rich phase of the Triton X-114-extracted RM or the soluble (*S*) and membrane protein (*P*) fractions of alkali-extracted RM. *D*, labeling of UV-irradiated ER membrane protein fractions via the [^{32}P]pCp/T4 RNA ligase protocol is ligase-dependent (lane 2) and reveals RNA-binding ER membrane proteins common to Triton X-114 (*TX-114*; *lane 3*) and alkali-extracted (*lane 4*) RM.

Proteomic Analyses of Cytosolic and ER-bound Polysomes Identifies Candidate ER-mRNA-anchoring Proteins—The molecular characteristics of the endomembrane protein-encoding mRNAs described above and in past studies (12, 13, 15) suggested a number of strategies for the identification of ER-integral membrane RNA-anchoring proteins, and three such strategies were used here. In one approach, we determined the Brij solubilization properties of a panel of HeLa ER-resident membrane proteins previously reported to function as ribosome-binding proteins and/or identified in a recent comprehensive "mRNA-interactome" screen in HeLa cells, as a means to identify candidate RNA-anchoring proteins in the BrR fraction (Fig. 5*A*) (60). Intriguingly, the ER membrane proteins examined displayed highly divergent Brij solubilization profiles. For example, Ire1α, an unfolded protein sensor and mRNA endonuclease (71); SRα, the SRP-interacting subunit of the SRP receptor (72); and reticulons 4b and 4c, which confer tubular ER membrane structure (73, 74), were highly enriched in the BrS fraction. SRα and reticulon 4a, the high molecular weight isoform of reticulons 4b and 4c, were recently identified as members of the HeLa mRNA interactome (60) and thus might contribute to mRNA-ER interactions in the BrS, but not BrR, fractions. The ribosome receptor p180 (RRBP1) was detected as two isoforms: 1) a 180-kDa form (p180) with reported ribosome receptor and microtubule binding activity (25, 75) and, more recently, described as a candidate general ER-poly(A) mRNA-binding protein (14) and 2) a 130-kDa form (ES130), which lacks the ribosome-binding decapeptide repeat motif but retains the coiled-coil microtubule binding domain (76). The two isoforms encode a common transmembrane domain, yet their Brij35 solubilization profiles were strikingly different, with ES130 partitioning to the BrS ER and p180 to the BrR ER.

Both isoforms contain the lysine-rich domain recently proposed to function in mRNA binding, which, although consistent with a role in general poly(A) mRNA anchoring to the ER, would be inconsistent with a selective endomembrane mRNA anchoring function. p180/ES130 was not, however, identified as either a validated or candidate RBP in the HeLa mRNA inter-

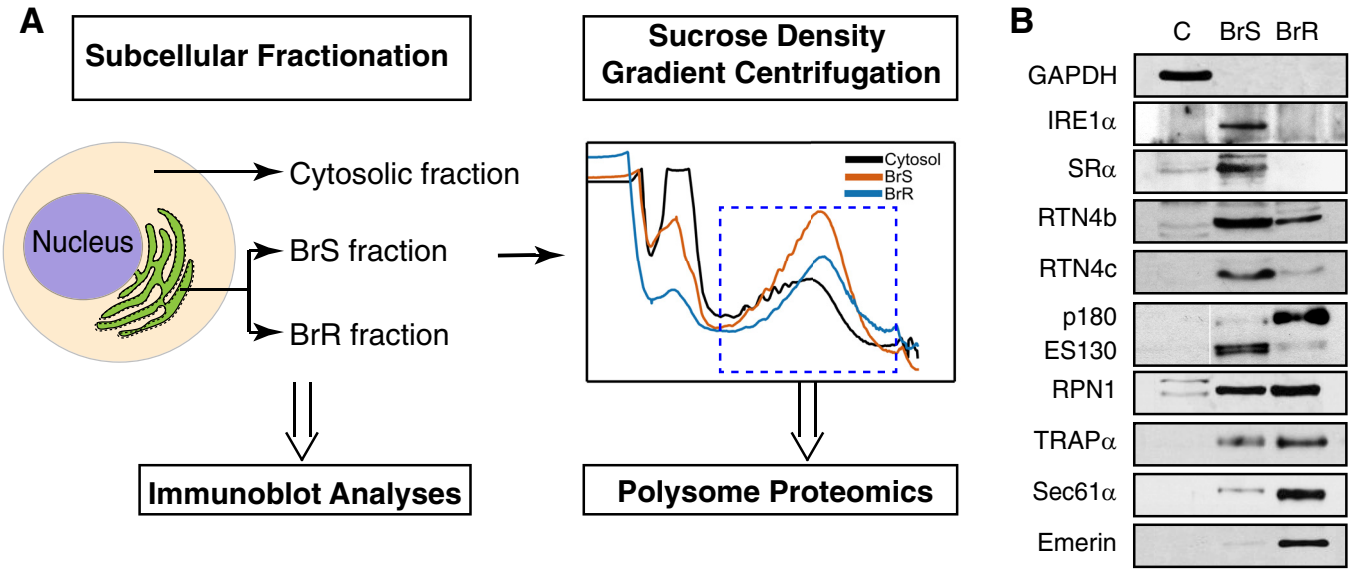

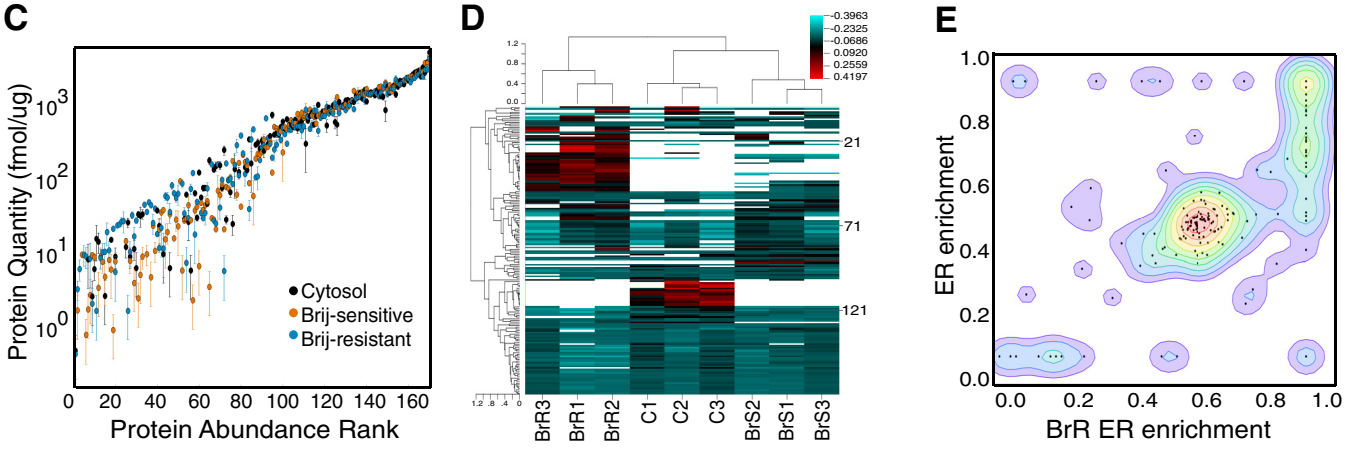

F

Protein	Name	Function	Proteomic quant. %Cyt	%BrS	%BrS	Western blot Cyt	BrS	BrR
		General polysome						
GBLP	Guanine nucleotide-binding protein beta-2	Signaling, translation regulation	36.8	32.4	30.8	ND		
PABP4	Polyadenylate-binding protein 4	Translation, mRNA binding	36.1	35.9	28.0			
RENT1	Regulator of nonsense transcripts 1	Nonsense mediated decay	24.8	38.1	37.1			
IF6	Eukaryotic translation initiation factor 6	80S assembly	25.1	34.8	40.1			
		Cytosol enriched						
G3P	Glyceraldehyde-3-phosphate dehydrogenase	Glycolysis, RNA binding	79.6	20.3	0.0			
NACA	Nascent polypeptide-associated complex subunit alpha	Suppress ER targeting	70.8	29.2	0.0	ND		
		ER enriched						
RPN1	Ribophorin 1	Glycosylation, ribosome binding	0.0	50.9	49.1	ND		
IF4A3	Eukaryotic initiation factor 4A-III	Exon junction complex	6.0	26.8	67.2			
PININ	Pinin	Exon junction complex	0.0	0.0	100.0	ND		
S61A1	Protein transport protein Sec61 subunit alpha	Protein translocation	0.0	0.0	100.0			
SC61B	Protein transport protein Sec61 subunit beta	Protein translocation	0.0	0.0	100.0			
GRP78	78 kDa glucose-regulated protein (BiP)	ER lumen chaperone	0.0	20.8	79.2			
CKAP4	Cytoskeleton-associated protein 4	ER microtubule anchoring	0.0	21.7	78.2	ND		

actome (60). Consistent with these findings, shRNA-mediated stable knockdown of p180/ES130 in HeLa cells did not reduce ER-associated calreticulin mRNA levels (data not shown). The lack of a discernible effect of p180 knockdown on ER-mRNA binding may reflect redundancies in anchoring mechanisms and/or cell type-specific functions of p180 and is under further study.

Ribophorin I (RPN1), a subunit of the oligosaccharyltransferase complex, and TRAPα (SSR1) reside in close physical proximity to ER-bound ribosomes (77–79). Ribophorin I was recently identified as a HeLa RBP, and TRAPα was identified as a candidate HeLa RBP; both proteins were distributed between the BrS and BrR fractions and enriched in the BrR fraction and therefore were scored as candidate ER-mRNA-anchoring proteins (60). Sec61α, the primary ER ribosome receptor and protein conducting channel component (53, 80) was highly enriched in the BrR fraction (Fig. 5*B*). Similar to TRAPα, Sec61α was identified as a candidate HeLa RBP (60). Interestingly, Sec61β, a subunit of the Sec61 complex, was also identified as a HeLa RBP (60), suggestive of a candidate mRNA anchor function for the Sec61 complex. Intriguingly, all three proteins are members of hetero-oligomeric complexes and have established functions in post-translational protein modification, protein translocation, and/or ribosome binding yet do not encode canonical RNA binding motifs (53, 68, 78, 79, 82). Emerin, an inner nuclear envelope protein integral membrane protein, was included as an additional control and was recovered uniquely in the BrR fraction.

In a parallel series of experiments, we performed a quantitative "polysome-interactome" screen for proteins that associate with cytosolic, BrS-derived, and/or BrR-derived polysomes. Here, triplicate independent cell fractionation experiments were performed, where polysomes from the cytosol, BrS, and BrR fractions were purified using a sucrose density gradient, and their protein compositions were analyzed by quantitative two-dimensional LC/MS/MS (Fig. 5, *C–F*, and supplemental Table S2). In this experiment, we sought to selectively capture biochemically stable (*e.g.* resistant to high salt, EDTA, and/or Brij35 solubilization) mRNA-protein interactions characteristic of the endomembrane protein mRNAs (13, 15). A modification of the absolute quantification two-dimensional LC/MS/MS methods developed by Silva and Geromanos was used for protein quantification (40, 41, 83). In this method, samples are added to protein standards, with the mass spectrometric signal response from the trypsin-generated, protein standard-derived peptides providing a signal response factor (counts/mol of protein) that is then used to determine the concentrations of identified proteins.

The primary features of this data set are summarized in Fig. 5, *C–E*, with the complete data set included in supplemental Table S2. The MS analysis yielded the identification of 283 proteins identified at high confidence (>2 peptides), with 3433 peptides providing spectral data for identification and quantification. The quantitative data represented in Fig. 5*C* are limited to those proteins that were identified and quantified in at least two of the three independent biological replicates. This additional selection reduced the number of proteins analyzed to 238. Polysome protein compositions of the three fractions were quite similar for the high abundance proteins composed predominately of ribosomal proteins but showed significant compositional divergence for the lower abundance proteins that include RBPs and ER membrane proteins. A hierarchical clustering analysis of these data is shown in Fig. 5*D* and demonstrates the high similarities between the individual sample replicates as well as the subcellular variations in polysome composition, where the BrR-derived polysomes were the most divergent, and the cytosol- and BrS-derived polysomes were the most similar. These data further highlight the distinct biochemical composition of the BrR ER-associated polysomes as detailed below.

To focus on polysome-interacting proteins enriched in the BrR, enrichment profiles were determined, where we examined the relative partitioning of identified proteins in the total ER (BrR + BrS) polysomes *versus* enrichment in the BrR polysomes (Fig. 5*E*). Here we note that those proteins that are highly enriched in the ER are also highly enriched in the BrR polysome fraction (Fig. 5*E*, *top right quadrant*). Conversely, the BrS polysomes display proteins that are either not ER-enriched (Fig. 5*E*, *bottom left quadrant*) or are present in both BrS and BrR fractions. Thus, the BrR polysomes possess more proteins that are unique to the ER, whereas BrS polysomes are more accurately described as generic; they are representative of the median polysome protein composition and translate a large fraction of the transcriptome. Notably, the prominent protein cluster at 0.66 ER enrichment is predominantly ribosomal proteins, which are largely common to both the ER-associated polysome fractions. In comparing the BrR and BrS polysomes, particularly striking differences were noted in the enrichments of ER membrane proteins, exon-junction complex (EJC), and nonsense-mediated decay components (Fig. 5*F*), and these findings are presented below.

In Fig. 5*F* are listed selected categories of polysome-associated proteins and their relative subcellular distributions in the cytosolic (*C*) and BrS- and BrR-derived polysomes. ER-resident membrane proteins identified in this analysis (Sec61α, Sec61β, and ribophorin I) are members of the candidate ER-mRNA-

FIGURE 5. **Quantitative "polysome interactor" screen reveals compartmentalized polysome-interacting protein distributions.** *A*, schematic of experimental design of polysome interactor screen. HeLa cells were fractionated to yield cytosol and BrS and BrR ER compartments. Polysome fractions were purified by sucrose gradient velocity sedimentation, and the heavy polysome fractions were selected for quantitative proteomic analysis. *B*, cytosol, BrS, and BrR fractions were analyzed by immunoblot for the indicated candidate ER membrane RNA-binding proteins. *C*, protein abundance rank distribution plot demonstrating high similarities in the abundant proteins and divergent compositions of lower abundance proteins in the cytosol, BrS, and BrR polysome fractions. *D*, heat map of compositional divergence of cytosol and ER-derived polysomes. The heat map illustrates the protein compositional similarities between the triplicate experimental datasets. The cytosol and Brij-sensitive ER fractions were most similar, and the Brij-resistant ER fraction was the most divergent. *E*, contour map of protein enrichment on the ER as a function of enrichment in the BrR ER, illustrating that the BrR-resistant ER fraction is more uniquely representative of the ER. *F*, tabulated data highlighting the primary features of the "polysome-interactor" screen data. Included in the figure are paired immunoblot analyses of protein distribution for a subset of the quantified proteins. A full listing of all identified proteins and their quantitative fractional enrichments is provided as supplemental Table S2. *ND*, not determined.

anchoring proteins proposed above and previously identified as members of the HeLa mRNA interactome or as candidate HeLa RBPs (60). In addition, the relative ER distributions identified in the Brij35 solubilization profile experiments (Fig. 5*B*) were closely mirrored in the polysome-interactome analysis, with the two Sec61 subunits being uniquely recovered in the BrR-derived polysome fraction and ribophorin I being recovered in both the BrS- and BrR-derived polysome fractions. These data thus identify a subset of ER membrane proteins that are selectively bound, directly or indirectly, to the BrR-derived polysomes and thus represent candidate selective ER-mRNA-anchoring proteins.

In the category "General Polysome," the fractional distributions of guanine nucleotide-binding protein β2 (RACK1), a prominent ribosome-associated protein, poly(A)-binding protein 4 (PABP1), UPF1 (RENT1), and eIF6 were similar between the three polysome fractions and serve as internal validation of the quantitative proteomic approach. For the category "Cytosol-enriched," we highlight two proteins, GAPDH, which was recently identified as an mRNA-binding protein, and the nascent chain-associated complex, which participates in protein folding and protein targeting to the ER. In the category "ER-enriched," we identified the core exon junction complex component eIF4AIII as highly enriched on ER-associated polysomes. The remaining EJC core components Magoh, Y14, and Barentz were not identified. Because this analysis is limited to polysome-recruited mRNAs, the absence of Magoh, Y14, and Barentz may reflect the release of these factors upon translation and/or EJC remodeling, as reported previously (84, 85). EJC interacting proteins with similar, ER-enriched subcellular distributions included Pinin and ACINU. That these proteins were identified on translationally active polysomes is suggestive of cytosolic functions complementary to their established roles in nonsense-mediated decay; such functions could include roles in mRNA localization and/or anchoring to the ER. The enrichment of EJC and splicing factors in the HeLa BrR-derived polysome fraction did, however, raise the concern of cross-contamination with nucleus-derived mRNA-splicing complexes. To determine whether the BrR polysome fraction contained nucleus-derived splicing complexes, we screened for nuclear integrity/spliceosome release at each stage of the cell fractionation procedure. We found that the nuclear envelope integrity was disrupted at the Brij35 solubilization stage, yielding release of the nuclear proteins histone H3F3A, HnRNPA1, and HuR into the BrS fraction (data not shown) and indicating that passive contamination of the BrR fraction by nuclear components was unlikely. As well, Brij35 treatment yielded the release of U2 and U4 snRNAs, both of which were recovered in the slowly migrating region of a velocity sedimentation experiment, separated from the polysome fraction (data not shown). These data provide additional support for the conclusion that the subset of EJC/nonsense-mediated decay proteins co-purifying with the BrR polysomes are in fact polysome-associated. Whether or not they participate in mRNA anchoring to the ER is unknown; it is equally plausible that they are associated with newly exported mRNAs that undergo selective translation on ER-associated ribosomes. In summary, the results of the polysome-interactome screen support a model where the ER-mRNA transcriptome is composed of populations of functionally related mRNAs bearing distinct RBP "fingerprints," which are anchored to the ER by distinct mechanisms.

Of the candidate ER-mRNA-anchoring proteins identified in the polysome-interactome screen, both Sec61α and ribophorin I have been previously reported to function as ribosome receptors (53, 86). Their identification in a polysome-interactor proteomic screen could, therefore, reflect ribosome rather than mRNA binding function (53, 86). For this reason, a third independent experimental approach was developed. Here, we again utilized canine pancreas RM as the source of ER-associated polysomes, reasoning that if the nuclear proteins identified in the HeLa polysome interactome screen were derived from cross-contamination, they would be largely absent from the ER-associated mRNPs. To address the question of mRNA *versus* rRNA binding activity, purified RM-derived polysomes were adjusted to 10 mM EDTA to dissociate the ribosomal subunits and their associated mRNAs (87) and the rRNA-free poly(A) mRNPs purified by native affinity chromatography on oligo(dT) in the presence of 10 mM EDTA (Fig. 6*A*). As an additional specificity control, identical quantities of ER-derived polysomes were digested with staphylococcal nuclease prior to oligo(dT) chromatography, and the nuclease-digested fraction was processed in parallel. A proteomic analysis was then conducted on the fractions eluted in low salt/formamide buffers, elution conditions selective for mRNA release (Fig. 6*B*).

The protein composition of the ribonucleoproteins purified by native oligo(dT) chromatography was determined by mass spectrometry of in-gel digested gel fragments (one-dimensional SDS-PAGE/LC/MS/MS). These results are summarized in Fig. 6*B*, with a full listing included in supplemental Table S3, and are limited to those proteins that were identified in at least two of three independent experiments, absent from the staphylococcal nuclease-treated controls, and whose identification was determined at high accuracy ($p < 0.05$, peptide count ≥ 2). In total, 170 proteins were identified, with 72 proteins meeting all criteria for selection.

As detailed in supplemental Table S3, 26 ribosomal proteins were identified, including proteins of the large and small ribosomal subunits. Of the 26 identified here, 18 were previously identified in the HeLa mRNA interactome and thus are likely to undergo direct interactions with poly(A) mRNAs (60). When compared with the HeLa polysome-interactome screen, this analysis yielded a substantially higher number of RNA-binding proteins and translation factors, reflecting the additional proteomic depth achieved by analyzing ribosome-free mRNPs. As summarized in Fig. 6*B*, nearly all proteins identified as native poly(A) mRNA interactors in the canine ER-associated mRNP screen were also identified in a recent HeLa mRNA interactome study (60). That we were able to identify this diversity of RBPs under native conditions demonstrates that these RBPs are stably bound to their target mRNAs.

The native mRNA interactome of the ER-associated poly(A) mRNA pool includes the EJC/nonsense-mediated decay factors eIF4AIII and UPF1, further corroborating the identification of these proteins in the ER-associated HeLa polysomes and providing additional independent evidence that these proteins can stably associate with ribosome-engaged mRNAs. A substantial number of the small nuclear ribonucleoproteins and heteroge-

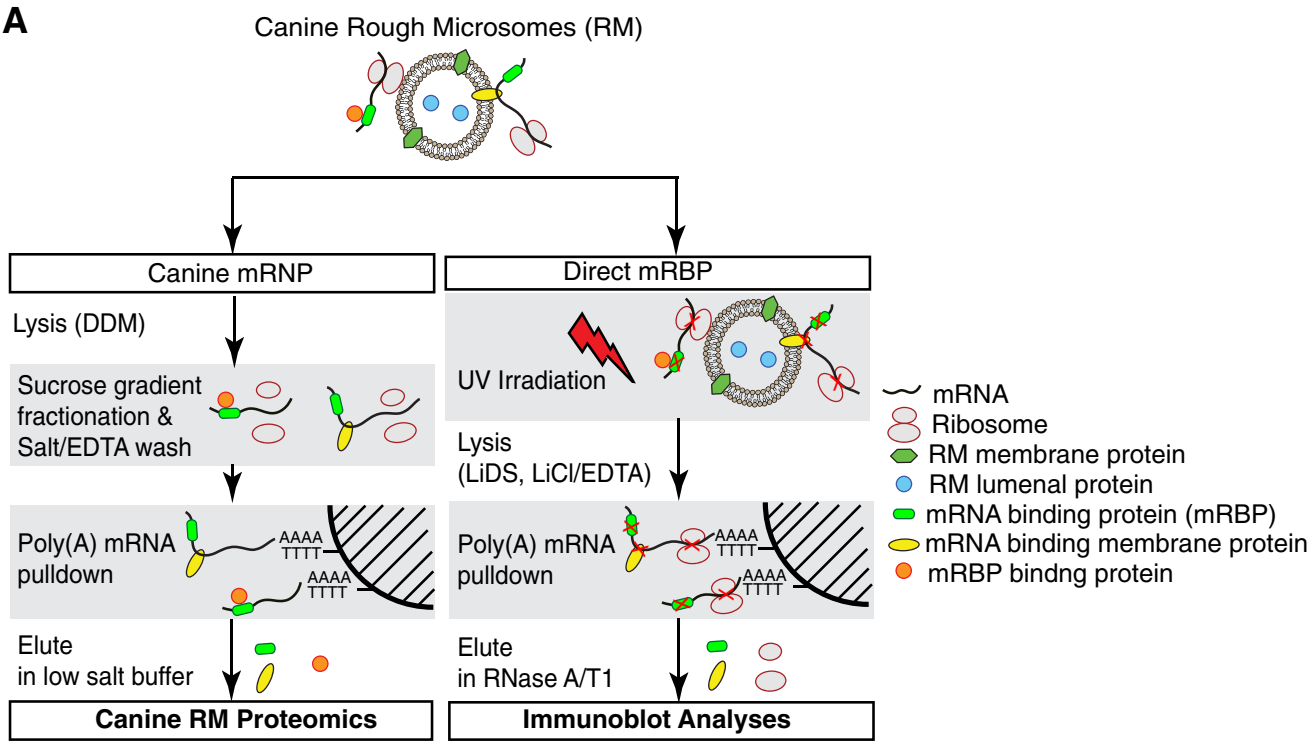

B

Canine mRNP	Name	Peptide count	HeLa mRNP (% in DDM)
RRBP1	Ribosome-binding protein 1 (p180)	88	ND
RPN2	Ribophorin 2	37	ND
MOGS	Mannosyl-oligosaccharide glucosidase	34	ND
SRPR	Signal recognition particle receptor subunit beta (SRβ)	34	ND
S61A1	Sec61 subunit alpha isoform 1(Sec61α)	20	100.0%
LRC59	Leucine-rich repeat-containing protein 59 (LRRC59)	20	ND
DGAT1	Diacylglycerol O-acyltransferase 1	18	ND
SRPRB	Signal recognition particle receptor subunit alpha (SRα)	17	ND
STT3A	Oligosaccharyl transferase subunit STT3A	15	ND
RPN1	Ribophorin 1	14	49.1%
LYRIC	Lysine-rich CEACAM1 co-isolated protein	14	ND
TRAM1	Translocating chain-associated membrane protein 1	11	ND
OST48	Oligosaccharyl transferase 48 kDa subunit	10	ND
PREB	Prolactin regulatory element-binding protein	10	ND
SSRA	Translocon-associated protein subunit alpha (TRAPα)	9	ND
PTSS1	Phosphatidylserine synthase 1	8	ND
ALG5	Dolichyl-phosphate beta-glucosyltransferase	6	ND
SPCS2	Signal peptidase complex subunit 2	6	ND
SC61B	Sec61 subunit beta (Sec61β)	5	100.0%
CKAP4	Cytoskeleton-associated protein 4 (Climp-63) (p63)	5	54.5%
SPCS3	Signal peptidase complex subunit 3	5	ND

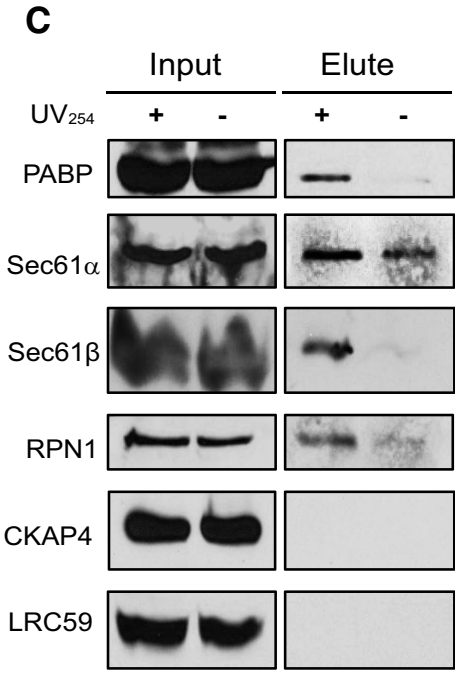

FIGURE 6. **Proteomic analysis of ER polysome-derived mRNPs identifies ER-mRNA interacting proteins.** *A*, schematic illustration of experimental protocol. In the left arm, rough microsomes were detergent-solubilized, the polysome fraction was isolated by sucrose gradient velocity sedimentation and treated with EDTA to release associated ribosomes, and the poly(A) mRNPs were chromatographed on Oligo(dT)-Cellulose Type 7. In the right arm, RM were UV-irradiated and lysed in Li-SDS, and protein-poly(A) adducts were purified on Oligo(dT)-Cellulose Type 7 in the presence of Li-SDS. *B*, partial listing of identified proteins at high confidence ($p \leq 0.05$), with paired comparisons with the HeLa mRNA interactome database as well as the HeLa "polysome interactor screen." *C*, RM were subjected to UV photocross-linking, the membranes were solubilized in Li-SDS, and poly(A) mRNAs were purified by oligo(dT) chromatography in Li-SDS. RNA-bound proteins were eluted by nuclease digestion, and the eluted fraction was analyzed by immunoblot.

neous nuclear ribonucleoproteins identified in our HeLa polysome interactome screen and in the HeLa mRNA interactome were also identified as interactors in the canine RM-derived mRNP analysis, so it can also be concluded that these proteins are present on translationally active, ER-associated polysomes and probably have functions extending beyond their roles in nonsense-mediated decay.

In a complementary series of experiments, RM were UV-irradiated to photocross-link bound mRNAs to their interacting protein partners, and the RM were then solubilized in lith-

ium SDS (Li-SDS). UV-cross-linked mRNA-protein complexes were purified by affinity chromatography on oligo(dT) in the presence of 0.5 M LiCl and Li-SDS, and mRNA-bound proteins were selectively eluted by the addition of RNase A/T1. The composition of this fraction was interrogated by immunoblot analysis (Fig. 6*C*). Of primary interest is the identification of Sec61α, Sec61β, and ribophorin I as poly(A) mRNA-associated ER membrane proteins. Importantly, other ER membrane proteins identified as mRNA-binding proteins in prior screens, such as CKAP4 and LRC59, were not detected in the nuclease eluate and thus may be mRNA-associated via indirect interactions. With respect to Sec61α, Sec61β, and ribophorin I, multiple, independent lines of experimental evidence now contribute to their identifications as mRNA-binding proteins and include, in addition to the data reported above, UV and 4-thiouridine photocross-linking, as reported in the HeLa mRNA interactome (60); selective enrichment on polysomes solubilized from the Brij-resistant ER of HeLa cells; and identification as native poly(A) mRNA-binding proteins of canine pancreas RM-derived mRNPs (Fig. 6*B*). In total, these data support a function for the Sec61 complex, subunits of the oligosaccharyltransferase complex, and, to a lesser degree, the translocon-associated protein complex in the direct anchoring of mRNAs to the ER. The identification of p180 in the RM, but not HeLa-derived fractions, is consistent with prior reports that p180 is highly expressed in terminally differentiated "professional" secretory cells but only very weakly in HeLa cells, where it did not meet statistical criteria for selection in the mRNA interactome or as a candidate RNA-binding protein (60, 76). Thus, we are unable to identify a role for p180 in the direct anchoring of endomembrane protein-encoding mRNAs to the HeLa ER, although a related function in terminally differentiated secretory cells remains plausible.

DISCUSSION

Studies in diverse organisms have revealed an extensive functional interplay between the processes of mRNA localization, translation, and decay and the ER (19, 88, 89). With recent genome-scale analyses demonstrating a broad representation of the mRNA transcriptome on the ER, there is now a pressing need to understand how mRNAs are selected, localized, and anchored to the ER. We address the latter question here, focusing on the mRNAs encoding the resident proteins of the endomembrane system, an essential gene family comprising over 500 genes and distinguished by a direct, ribosome-independent mode of membrane association (13, 15). Here we provide evidence that subunits of the Sec61 and oligosaccharyltransferase complexes function as ER-mRNA-anchoring proteins.

In microsomes, endomembrane protein-encoding mRNAs are distinguished from secretory protein-encoding mRNAs by their capacity to remain membrane-associated following extraction of bound ribosomes with high salt and/or EDTA (13, 15). This finding suggested a relatively simple biochemical distinction in the two ER-mRNA association mechanisms, where secretory protein-encoding mRNAs are anchored via their engagement on membrane-bound ribosomes, and endomembrane protein-encoding mRNAs engage in direct binding interactions with components of the ER. In semi-intact HeLa cells, this distinction was recapitulated by sequential detergent fractionation with detergents (Brij family) that selectively solubilize the glycerolphospholipid but not sphingolipid fraction of biological membranes.

Given the selective Brij sensitivity of ER-mRNA interactions, we thought it plausible that candidate integral membrane mRNA-anchoring proteins would also display heterogeneous distributions in the detergent-induced ER membrane domains, and in studies with a subset of ER-resident membrane proteins, this was confirmed. These observations, coupled with UV photocross-linking studies demonstrating a diverse population of integral membrane RNA-interacting proteins, suggested a model where mRNAs are selectively anchored via interactions with membrane proteins. Quantitative proteomic analysis of polyribsomes purified from the cytosol and the Brij-sensitive and Brij-resistant ER domains provided evidence for such a model; polysomes from the Brij-resistant HeLa ER were markedly enriched in mRNAs encoding resident ER, Golgi, and lysosomal proteins and were uniquely associated with the core translocon components Sec61α/β. These data support a model where the endomembrane-resident protein-encoding mRNAs are selectively and directly anchored to resident proteins of the ER. In such a model, core translocon components would function as RNA-organizing centers to enable a spatial organization of gene expression on the ER, a proposal consistent with the RNA operon model (90, 91).

At first glance, a role for translocon components in selective mRNA anchoring to the ER seems unlikely because it implies a selective function (mRNA anchoring) for proteins that perform a general function (protein translocation). However, the Sec61 and oligosaccharyltransferase complexes exist in different hetero-oligomeric states and are in stoichiometric excess to translocation sites (92, 93). It is thus reasonable to consider that these essential proteins may be multifunctional, where particular oligomeric forms function in mRNA and/or ribosome binding to the ER, and other forms serve as the protein translocation machinery.

A central question raised by these data is why direct RNA anchoring appears to be selective for the endomembrane protein-encoding mRNAs. In one view, a cohort-selective mRNA binding activity would provide a mechanism for coordinate biogenesis of the endomembrane system and/or "biogenesis domains" dedicated to preorganelle assembly, as has been proposed for peroxisome biogenesis (reviewed in Ref. 59). Such a model may be of particular relevance to the remarkable enrichment of lysosome-resident protein-encoding mRNAs in the Brij-resistant ER.

An additional question arising from this study concerns the mechanism of ribosome binding to the ER. Although a somewhat contentious question, there is general agreement that the Sec61 complex is the primary ER ribosome receptor (53, 94–96). A key observation leading to this assignment was that in native membranes, ribosome binding to Sec61 is highly salt-resistant (53). In the current study, we found that a substantial fraction of ER-bound polysomes are released in the presence of 0.5 M salt/Brij35, that these polysomes are enriched in mRNAs encoding cytosolic secretory cargo proteins, and in contrast to polysomes engaged in the translation of endomembrane pro-

tein-encoding mRNAs, the solubilized polysomes did not contain detectable quantities of Sec61 subunits. Such data imply that ribosomes, in an mRNA-dependent manner, might either bind to membrane receptors other than the Sec61 complex, or, alternatively, the ribosome-Sec61 binding interaction might vary as a function of the mRNA undergoing translation. Regardless, these data suggest that further investigation into the mechanism and diversity of ribosome association with the ER is needed.

In summary, we demonstrate that the mRNA infrastructure of the ER is complex, with endomembrane protein-encoding mRNAs undergoing selective association with components of the translocon. The challenge ahead is to determine the molecular mechanism(s) that enable the selective association of the endomembrane-resident protein mRNAs with their ER-resident membrane protein-binding partners. Curiously, although none of the interacting ER membrane proteins that we identify display the canonical RNA binding motifs identified in soluble RNA-binding proteins, they possess stretches of basic residues in cytosol-facing loops that could have selective RNA binding activity.

Given the large number of mRNAs that utilize a direct ER association mechanism and the established complexity of *cis*-encoded mRNA localization signals in even the best characterized mRNA localization examples (81), it seems unlikely that a common ER localization "zip code" would serve to direct mRNA localization to the ER. Consistent with this view, ER localization information has been demonstrated to reside in the transmembrane domain-coding region of placental alkaline phosphatase and, in the case of the yeast membrane protein Pmp1, a repeating UG-rich motif in the 3′-UTR (17, 22). Regardless of the apparent complexity, progress toward the identification of the RNA binding motifs present in these candidate RNA-anchoring proteins and the sequence/two-dimensional structural motifs they recognize will help to identify the molecular organization of the ER-mRNA infrastructure.

Acknowledgments—We thank Harold Erickson for conducting negative staining electron microscopy analyses and for enthusiastic interest. We are also grateful to Sam Johnson, Director of the Duke Light Microscopy Core facility, for thoughtful guidance and advice and the staff of the Duke Microarray core facility for assistance with the microarray studies. We thank Srinivas Ramachandran for helpful advice on the bioinformatic and statistical data analyses and Angeline S. L. Tay for critical reading of the manuscript. We thank Matthias Gromeier and Mariano Garcia-Blanco of Duke University for antisera to H3F3A and HnRNPA1, respectively, Riqiang Yan (Lerner Research Institute) for reticulon antisera, and Kiyoko Ogawa-Goto (Nippei Research Institute, Japan) for antisera to p180.

REFERENCES

1. Blobel, G. (2000) Protein targeting. *Biosci. Rep.* **20,** 303–344
2. Palade, G. (1975) Intracellular aspects of the process of protein synthesis. *Science* **189,** 347–358
3. Walter, P., and Johnson, A. E. (1994) Signal sequence recognition and protein targeting to the endoplasmic reticulum membrane. *Annu. Rev. Cell Biol.* **10,** 87–119
4. Suh, J., and Hutter, H. (2012) A survey of putative secreted and transmembrane proteins encoded in the *C. elegans* genome. *BMC Genomics* **13,** 333
5. Martin, K. C., and Ephrussi, A. (2009) mRNA localization: gene expression in the spatial dimension. *Cell* **136,** 719–730
6. Medioni, C., Mowry, K., and Besse, F. (2012) Principles and roles of mRNA localization in animal development. *Development* **139,** 3263–3276
7. Blobel, G., Walter, P., Chang, C. N., Goldman, B. M., Erickson, A. H., and Lingappa, V. R. (1979) Translocation of proteins across membranes: the signal hypothesis and beyond. *Symp. Soc. Exp. Biol.* **33,** 9–36
8. Zimmermann, R., Eyrisch, S., Ahmad, M., and Helms, V. (2011) Protein translocation across the ER membrane. *Biochim. Biophys. Acta* **1808,** 912–924
9. Diehn, M., Eisen, M. B., Botstein, D., and Brown, P. O. (2000) Large-scale identification of secreted and membrane-associated gene products using DNA microarrays. *Nat. Genet.* **25,** 58–62
10. Lerner, R. S., Seiser, R. M., Zheng, T., Lager, P. J., Reedy, M. C., Keene, J. D., and Nicchitta, C. V. (2003) Partitioning and translation of mRNAs encoding soluble proteins on membrane-bound ribosomes. *RNA* **9,** 1123–1137
11. Nicchitta, C. V., Lerner, R. S., Stephens, S. B., Dodd, R. D., and Pyhtila, B. (2005) Pathways for compartmentalizing protein synthesis in eukaryotic cells: the template-partitioning model. *Biochem. Cell Biol.* **83,** 687–695
12. Reid, D. W., and Nicchitta, C. V. (2012) Primary role for endoplasmic reticulum-bound ribosomes in cellular translation identified by ribosome profiling. *J. Biol. Chem.* **287,** 5518–5527
13. Chen, Q., Jagannathan, S., Reid, D. W., Zheng, T., and Nicchitta, C. V. (2011) Hierarchical regulation of mRNA partitioning between the cytoplasm and the endoplasmic reticulum of mammalian cells. *Mol. Biol. Cell* **22,** 2646–2658
14. Cui, X. A., Zhang, H., and Palazzo, A. F. (2012) p180 promotes the ribosome-independent localization of a subset of mRNA to the endoplasmic reticulum. *PLoS Biol.* **10,** e1001336
15. Pyhtila, B., Zheng, T., Lager, P. J., Keene, J. D., Reedy, M. C., and Nicchitta, C. V. (2008) Signal sequence- and translation-independent mRNA localization to the endoplasmic reticulum. *RNA* **14,** 445–453
16. Kraut-Cohen, J., Afanasieva, E., Haim-Vilmovsky, L., Slobodin, B., Yosef, I., Bibi, E., and Gerst, J. E. (2013) Translation- and SRP-independent mRNA targeting to the endoplasmic reticulum in the yeast Saccharomyces cerevisiae. *Mol. Biol. Cell* **24,** 3069–3084
17. Loya, A., Pnueli, L., Yosefzon, Y., Wexler, Y., Ziv-Ukelson, M., and Arava, Y. (2008) The 3′-UTR mediates the cellular localization of an mRNA encoding a short plasma membrane protein. *RNA* **14,** 1352–1365
18. Nevo-Dinur, K., Nussbaum-Shochat, A., Ben-Yehuda, S., and Amster-Choder, O. (2011) Translation-independent localization of mRNA in *E. coli*. *Science* **331,** 1081–1084
19. Kraut-Cohen, J., and Gerst, J. E. (2010) Addressing mRNAs to the ER: cis sequences act up! *Trends Biochem. Sci.* **35,** 459–469
20. Glisovic, T., Bachorik, J. L., Yong, J., and Dreyfuss, G. (2008) RNA-binding proteins and post-transcriptional gene regulation. *FEBS Lett.* **582,** 1977–1986
21. Lunde, B. M., Moore, C., and Varani, G. (2007) RNA-binding proteins: modular design for efficient function. *Nat. Rev. Mol. Cell Biol.* **8,** 479–490
22. Cui, X. A., Zhang, Y., Hong, S. J., and Palazzo, A. F. (2013) Identification of a region within the placental alkaline phosphatase mRNA that mediates p180-dependent targeting to the endoplasmic reticulum. *J. Biol. Chem.* **288,** 29633–29641
23. Bai, J. Z., Leung, E., Holloway, H., and Krissansen, G. W. (2008) Alternatively spliced forms of the P180 ribosome receptor differ in their ability to induce the proliferation of rough endoplasmic reticulum. *Cell Biol. Int.* **32,** 473–483
24. Ogawa-Goto, K., Irie, S., Omori, A., Miura, Y., Katano, H., Hasegawa, H., Kurata, T., Sata, T., and Arao, Y. (2002) An endoplasmic reticulum protein, p180, is highly expressed in human cytomegalovirus-permissive cells and interacts with the tegument protein encoded by UL48. *J. Virol.* **76,** 2350–2362
25. Ogawa-Goto, K., Tanaka, K., Ueno, T., Tanaka, K., Kurata, T., Sata, T., and Irie, S. (2007) p180 is involved in the interaction between the endoplasmic reticulum and microtubules through a novel microtubule-binding and bundling domain. *Mol. Biol. Cell* **18,** 3741–3751
26. Ueno, T., Kaneko, K., Sata, T., Hattori, S., and Ogawa-Goto, K. (2012) Regulation of polysome assembly on the endoplasmic reticulum by a

coiled-coil protein, p180. *Nucleic Acids Res.* **40,** 3006–3017
27. Ueno, T., Tanaka, K., Kaneko, K., Taga, Y., Sata, T., Irie, S., Hattori, S., and Ogawa-Goto, K. (2010) Enhancement of procollagen biosynthesis by p180 through augmented ribosome association on the endoplasmic reticulum in response to stimulated secretion. *J. Biol. Chem.* **285,** 29941–29950
28. Jagannathan, S., Nwosu, C., and Nicchitta, C. V. (2011) Analyzing mRNA localization to the endoplasmic reticulum via cell fractionation. *Methods Mol. Biol.* **714,** 301–321
29. Stephens, S. B., and Nicchitta, C. V. (2007) *In vitro* and tissue culture methods for analysis of translation initiation on the endoplasmic reticulum. *Methods Enzymol.* **431,** 47–60
30. Stephens, S. B., and Nicchitta, C. V. (2008) Divergent regulation of protein synthesis in the cytosol and endoplasmic reticulum compartments of mammalian cells. *Mol. Biol. Cell* **19,** 623–632
31. Milam, S. L., Osawa, M., and Erickson, H. P. (2012) Negative-stain electron microscopy of inside-out FtsZ rings reconstituted on artificial membrane tubules show ribbons of protofilaments. *Biophys. J.* **103,** 59–68
32. Chomczynski, P., and Sacchi, N. (2006) The single-step method of RNA isolation by acid guanidinium thiocyanate-phenol-chloroform extraction: twenty-something years on. *Nat. Protoc.* **1,** 581–585
33. Bordier, C. (1981) Phase separation of integral membrane proteins in Triton X-114 solution. *J. Biol. Chem.* **256,** 1604–1607
34. Nicchitta, C. V., and Blobel, G. (1993) Lumenal proteins of the endoplasmic reticulum are required to complete protein translocation. *Cell* **73,** 989–998
35. Gilar, M., Olivova, P., Daly, A. E., and Gebler, J. C. (2005) Orthogonality of separation in two-dimensional liquid chromatography. *Anal. Chem.* **77,** 6426–6434
36. Gilar, M., Olivova, P., Daly, A. E., and Gebler, J. C. (2005) Two-dimensional separation of peptides using RP-RP-HPLC system with different pH in first and second separation dimensions. *J. Sep. Sci.* **28,** 1694–1703
37. Dowell, J. A., Frost, D. C., Zhang, J., and Li, L. (2008) Comparison of two-dimensional fractionation techniques for shotgun proteomics. *Anal. Chem.* **80,** 6715–6723
38. Keller, A., Nesvizhskii, A. I., Kolker, E., and Aebersold, R. (2002) Empirical statistical model to estimate the accuracy of peptide identifications made by MS/MS and database search. *Anal. Chem.* **74,** 5383–5392
39. Nesvizhskii, A. I., Keller, A., Kolker, E., and Aebersold, R. (2003) A statistical model for identifying proteins by tandem mass spectrometry. *Anal. Chem.* **75,** 4646–4658
40. Silva, J. C., Denny, R., Dorschel, C., Gorenstein, M. V., Li, G. Z., Richardson, K., Wall, D., and Geromanos, S. J. (2006) Simultaneous qualitative and quantitative analysis of the *Escherichia coli* proteome: a sweet tale. *Mol. Cell. Proteomics* **5,** 589–607
41. Silva, J. C., Gorenstein, M. V., Li, G. Z., Vissers, J. P., and Geromanos, S. J. (2006) Absolute quantification of proteins by LCMSE: a virtue of parallel MS acquisition. *Mol. Cell. Proteomics* **5,** 144–156
42. Saka, H. A., Thompson, J. W., Chen, Y. S., Kumar, Y., Dubois, L. G., Moseley, M. A., and Valdivia, R. H. (2011) Quantitative proteomics reveals metabolic and pathogenic properties of *Chlamydia trachomatis* developmental forms. *Mol. Microbiol.* **82,** 1185–1203
43. Wilm, M., Shevchenko, A., Houthaeve, T., Breit, S., Schweigerer, L., Fotsis, T., and Mann, M. (1996) Femtomole sequencing of proteins from polyacrylamide gels by nano-electrospray mass spectrometry. *Nature* **379,** 466–469
44. Rapoport, T. A., Wiedmann, M., Kurzchalia, T. V., and Hartmann, E. (1989) Signal recognition in protein translocation across the endoplasmic reticulum membrane. *Biochem. Soc. Trans.* **17,** 325–328
45. Cardelli, J., Long, B., and Pitot, H. C. (1976) Direct association of messenger RNA labeled in the presence of fluoroorotate with membranes of the endoplasmic reticulum in rat liver. *J. Cell Biol.* **70,** 47–58
46. Kruppa, J., and Sabatini, D. D. (1977) Release of poly A^+ messenger RNA from rat liver rough microsomes upon disassembly of bound polysomes. *J. Cell Biol.* **74,** 414–427
47. Lodish, H. F., and Froshauer, S. (1977) Binding of viral glycoprotein mRNA to endoplasmic reticulum membranes is disrupted by puromycin. *J. Cell Biol.* **74,** 358–364
48. Beckers, C. J., Keller, D. S., and Balch, W. E. (1987) Semi-intact cells permeable to macromolecules: use in reconstitution of protein transport from the endoplasmic reticulum to the Golgi complex. *Cell* **50,** 523–534
49. Stephens, S. B., Dodd, R. D., Lerner, R. S., Pyhtila, B. M., and Nicchitta, C. V. (2008) Analysis of mRNA partitioning between the cytosol and endoplasmic reticulum compartments of mammalian cells. *Methods Mol. Biol.* **419,** 197–214
50. Freidlin, P. J., and Patterson, R. J. (1980) Heparin releases monosomes and polysomes from rough endoplasmic reticulum. *Biochem. Biophys. Res. Commun.* **93,** 521–527
51. Lande, M. A., Adesnik, M., Sumida, M., Tashiro, Y., and Sabatini, D. D. (1975) Direct association of messenger RNA with microsomal membranes in human diploid fibroblasts. *J. Cell Biol.* **65,** 513–528
52. Veis, A., Leibovich, S. J., Evans, J., and Kirk, T. Z. (1985) Supramolecular assemblies of mRNA direct the coordinated synthesis of type I procollagen chains. *Proc. Natl. Acad. Sci. U.S.A.* **82,** 3693–3697
53. Görlich, D., Prehn, S., Hartmann, E., Kalies, K. U., and Rapoport, T. A. (1992) A mammalian homolog of SEC61p and SECYp is associated with ribosomes and nascent polypeptides during translocation. *Cell* **71,** 489–503
54. Schuck, S., Honsho, M., Ekroos, K., Shevchenko, A., and Simons, K. (2003) Resistance of cell membranes to different detergents. *Proc. Natl. Acad. Sci. U.S.A.* **100,** 5795–5800
55. Simons, K., and Toomre, D. (2000) Lipid rafts and signal transduction. *Nat. Rev. Mol. Cell Biol.* **1,** 31–39
56. Raj, A., van den Bogaard, P., Rifkin, S. A., van Oudenaarden, A., and Tyagi, S. (2008) Imaging individual mRNA molecules using multiple singly labeled probes. *Nat. Methods* **5,** 877–879
57. Pagano, R. E., Martin, O. C., Kang, H. C., and Haugland, R. P. (1991) A novel fluorescent ceramide analogue for studying membrane traffic in animal cells: accumulation at the Golgi apparatus results in altered spectral properties of the sphingolipid precursor. *J. Cell Biol.* **113,** 1267–1279
58. Axelsson, M. A., and Warren, G. (2004) Rapid, endoplasmic reticulum-independent diffusion of the mitotic Golgi haze. *Mol. Biol. Cell* **15,** 1843–1852
59. Dimitrov, L., Lam, S. K., and Schekman, R. (2013) The role of the endoplasmic reticulum in peroxisome biogenesis. *Cold Spring Harb. Perspect. Biol.* **5,** a013243
60. Castello, A., Fischer, B., Eichelbaum, K., Horos, R., Beckmann, B. M., Strein, C., Davey, N. E., Humphreys, D. T., Preiss, T., Steinmetz, L. M., Krijgsveld, J., and Hentze, M. W. (2012) Insights into RNA biology from an atlas of mammalian mRNA-binding proteins. *Cell* **149,** 1393–1406
61. Hogan, D. J., Riordan, D. P., Gerber, A. P., Herschlag, D., and Brown, P. O. (2008) Diverse RNA-binding proteins interact with functionally related sets of RNAs, suggesting an extensive regulatory system. *PLoS Biol.* **6,** e255
62. Song, Y., Jiang, Y., Ying, W., Gong, Y., Yan, Y., Yang, D., Ma, J., Xue, X., Zhong, F., Wu, S., Hao, Y., Sun, A., Li, T., Sun, W., Wei, H., Zhu, Y., Qian, X., and He, F. (2010) Quantitative proteomic survey of endoplasmic reticulum in mouse liver. *J. Proteome Res.* **9,** 1195–1202
63. Tsvetanova, N. G., Klass, D. M., Salzman, J., and Brown, P. O. (2010) Proteome-wide search reveals unexpected RNA-binding proteins in *Saccharomyces cerevisiae*. *PloS One* **5,** e12671
64. Pashev, I. G., Dimitrov, S. I., and Angelov, D. (1991) Crosslinking proteins to nucleic acids by ultraviolet laser irradiation. *Trends Biochem. Sci.* **16,** 323–326
65. Walter, P., and Blobel, G. (1983) Preparation of microsomal membranes for cotranslational protein translocation. *Methods Enzymol.* **96,** 84–93
66. Kikuchi, Y., Hishinuma, F., and Sakaguchi, K. (1978) Addition of mononucleotides to oligoribonucleotide acceptors with T4 RNA ligase. *Proc. Natl. Acad. Sci. U.S.A.* **75,** 1270–1273
67. Mathias, R. A., Chen, Y. S., Kapp, E. A., Greening, D. W., Mathivanan, S., and Simpson, R. J. (2011) Triton X-114 phase separation in the isolation and purification of mouse liver microsomal membrane proteins. *Methods* **54,** 396–406
68. Prinz, A., Behrens, C., Rapoport, T. A., Hartmann, E., and Kalies, K. U. (2000) Evolutionarily conserved binding of ribosomes to the translocation channel via the large ribosomal RNA. *EMBO J.* **19,** 1900–1906
69. Stalder, L., Heusermann, W., Sokol, L., Trojer, D., Wirz, J., Hean, J., Fritzsche, A., Aeschimann, F., Pfanzagl, V., Basselet, P., Weiler, J., Hinter-

steiner, M., Morrissey, D. V., and Meisner-Kober, N. C. (2013) The rough endoplasmatic reticulum is a central nucleation site of siRNA-mediated RNA silencing. *EMBO J.* **32,** 1115–1127
70. Trcek, T., Sato, H., Singer, R. H., and Maquat, L. E. (2013) Temporal and spatial characterization of nonsense-mediated mRNA decay. *Genes Dev.* **27,** 541–551
71. Sidrauski, C., and Walter, P. (1997) The transmembrane kinase Ire1p is a site-specific endonuclease that initiates mRNA splicing in the unfolded protein response. *Cell* **90,** 1031–1039
72. Gilmore, R., Blobel, G., and Walter, P. (1982) Protein translocation across the endoplasmic reticulum. I. Detection in the microsomal membrane of a receptor for the signal recognition particle. *J. Cell Biol.* **95,** 461–469
73. Shibata, Y., Voss, C., Rist, J. M., Hu, J., Rapoport, T. A., Prinz, W. A., and Voeltz, G. K. (2008) The reticulon and DP1/Yop1p proteins form immobile oligomers in the tubular endoplasmic reticulum. *J. Biol. Chem.* **283,** 18892–18904
74. Voeltz, G. K., Prinz, W. A., Shibata, Y., Rist, J. M., and Rapoport, T. A. (2006) A class of membrane proteins shaping the tubular endoplasmic reticulum. *Cell* **124,** 573–586
75. Savitz, A. J., and Meyer, D. (1990) Identification of a ribosome receptor in the rough endoplasmic reticulum. *Nature* **346,** 540–544
76. Langley, R., Leung, E., Morris, C., Berg, R., McDonald, M., Weaver, A., Parry, D. A., Ni, J., Su, J., Gentz, R., Spurr, N., and Krissansen, G. W. (1998) Identification of multiple forms of 180-kDa ribosome receptor in human cells. *DNA Cell Biol.* **17,** 449–460
77. Dejgaard, K., Theberge, J. F., Heath-Engel, H., Chevet, E., Tremblay, M. L., and Thomas, D. Y. (2010) Organization of the Sec61 translocon, studied by high resolution native electrophoresis. *J. Proteome Res.* **9,** 1763–1771
78. Hartmann, E., Görlich, D., Kostka, S., Otto, A., Kraft, R., Knespel, S., Bürger, E., Rapoport, T. A., and Prehn, S. (1993) A tetrameric complex of membrane proteins in the endoplasmic reticulum. *Eur. J. Biochem.* **214,** 375–381
79. Kelleher, D. J., Kreibich, G., and and Gilmore, R. (1992) Oligosaccharyltransferase activity is associated with a protein complex composed of ribophorins I and II and a 48 kDa protein. *Cell* **69,** 55–65
80. Beckmann, R., Spahn, C. M., Eswar, N., Helmers, J., Penczek, P. A., Sali, A., Frank, J., and Blobel, G. (2001) Architecture of the protein-conducting channel associated with the translating 80S ribosome. *Cell* **107,** 361–372
81. Hamilton, R. S., and Davis, I. (2011) Identifying and searching for conserved RNA localisation signals. *Methods Mol. Biol.* **714,** 447–466
82. Kelleher, D. J., and Gilmore, R. (2006) An evolving view of the eukaryotic oligosaccharyltransferase. *Glycobiology* **16,** 47R–62R
83. Silva, J. C., Denny, R., Dorschel, C. A., Gorenstein, M., Kass, I. J., Li, G. Z., McKenna, T., Nold, M. J., Richardson, K., Young, P., and Geromanos, S. (2005) Quantitative proteomic analysis by accurate mass retention time pairs. *Anal. Chem.* **77,** 2187–2200
84. Dostie, J., and Dreyfuss, G. (2002) Translation is required to remove Y14 from mRNAs in the cytoplasm. *Curr. Biol.* **12,** 1060–1067
85. Gehring, N. H., Lamprinaki, S., Kulozik, A. E., and Hentze, M. W. (2009) Disassembly of exon junction complexes by PYM. *Cell* **137,** 536–548
86. Kreibich, G., Ulrich, B. L., and Sabatini, D. D. (1978) Proteins of rough microsomal membranes related to ribosome binding. I. Identification of ribophorins I and II, membrane proteins characteristic of rough microsomes. *J. Cell Biol.* **77,** 464–487
87. Longuet, M., Auger-Buendia, M. A., and Tavitian, A. (1979) Studies on the distribution of ribosomal proteins in mammalian ribosomal subunits. *Biochimie* **61,** 1113–1123
88. Blower, M. D. (2013) Molecular insights into intracellular RNA localization. *Int. Rev. Cell Mol. Biol.* **302,** 1–39
89. Weil, D., and Hollien, J. (2013) Cytoplasmic organelles on the road to mRNA decay. *Biochim. Biophys. Acta* **1829,** 725–731
90. Morris, A. R., Mukherjee, N., and Keene, J. D. (2010) Systematic analysis of posttranscriptional gene expression. *Wiley Interdiscip. Rev. Syst. Biol. Med.* **2,** 162–180
91. Keene, J. D. (2007) RNA regulons: coordination of post-transcriptional events. *Nat. Rev. Genet.* **8,** 533–543
92. Guth, S., Völzing, C., Müller, A., Jung, M., and Zimmermann, R. (2004) Protein transport into canine pancreatic microsomes: a quantitative approach. *Eur. J. Biochem.* **271,** 3200–3207
93. Kelleher, D. J., Karaoglu, D., Mandon, E. C., and Gilmore, R. (2003) Oligosaccharyltransferase isoforms that contain different catalytic STT3 subunits have distinct enzymatic properties. *Mol. Cell* **12,** 101–111
94. Menetret, J. F., Neuhof, A., Morgan, D. G., Plath, K., Radermacher, M., Rapoport, T. A., and Akey, C. W. (2000) The structure of ribosome-channel complexes engaged in protein translocation. *Mol. Cell* **6,** 1219–1232
95. Morgan, D. G., Ménétret, J. F., Neuhof, A., Rapoport, T. A., and Akey, C. W. (2002) Structure of the mammalian ribosome-channel complex at 17 Å resolution. *J. Mol. Biol.* **324,** 871–886
96. Voorhees, R. M., Fernández, I. S., Scheres, S. H., and Hegde, R. S. (2014) Structure of the mammalian ribosome-Sec61 complex to 3.4 Å resolution. *Cell* **157,** 1632–1643